

# **Discovery of novel marine enzymes for inhibition of biofilm formation of pathogen strains**

## **Dissertation**

for obtaining the degree of  
Doctor rerum naturalium (Dr. rer. nat.)

at the Department of Biology  
Subdivision at the Faculty of Mathematics, Informatics and Natural Science  
of the University of Hamburg

submitted by  
**Marie Kristin Peters**

Hamburg, 2023

The following evaluators recommend the admission of the dissertation:

Prof. Dr. Wolfgang R. Streit

Dr. Ines Krohn

Day of oral defence: 10.11.2023

### **Eidesstattliche Versicherung**

Hiermit erkläre ich an Eides statt, dass ich die vorliegende Dissertationsschrift selbst verfasst und keine anderen als die angegebenen Quellen und Hilfsmittel benutzt habe.

### **Declaration on oath**

I hereby declare, on oath, that I have written the present dissertation by my own and have not used any other than the acknowledged resources and aids.

Buchholz, 20.07.2023

  
\_\_\_\_\_

Marie Kristin Peters

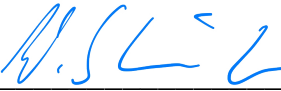
## Contribution to the quoted article


Peters M.K., Astafyeva Y., Han Y., Macdonald J.F.H., Indenbirken D., Nakel J., Viridi S, Westhoff G., Streit W.R., and Krohn I. (2023). „Novel marine metalloprotease – new approaches for inhibition of biofilm formation of *Stenotrophomonas maltophilia*.” Appl Microbiol Biotechnol **107**, 7119–7134, doi: 10.1007/s00253-023-12781-0.

Participating in planning, performance, and evaluation of all experimental work:

- Sampling of material and preparation of enrichment cultures
- DNA isolation and clean-up
- Biofilm plate assays
- Fluorescence microscopy
- Fractionation of samples via FPLC
- RNA isolation and preparation for sequencing

Participating in the design of the study and writing of the manuscript.

Hamburg, 20.07.2023,  \_\_\_\_\_  
Prof. Dr. Wolfgang R. Streit (Supervisor)

Hamburg, 20.07.2023,  \_\_\_\_\_  
Dr. Ines Krohn (Co-supervisor)

# Table of Contents

<b>Table of Contents</b> .....	I
<b>List of Figures</b> .....	IV
<b>List of Tables</b> .....	V
<b>List of Abbreviations</b> .....	VI
<b>Abstract</b> .....	VIII
<b>Zusammenfassung</b> .....	X
<b>1 Introduction</b> .....	1
1.1 Marine habitats as promising resources .....	1
1.2 Metagenomics as a tool for enzyme discovery .....	2
1.3 Secondary metabolites with medical applications .....	2
1.4 Microbial biofilms .....	3
1.5 Potential pathogenic bacterium <i>Stenotrophomonas maltophilia</i> .....	4
1.6 Aim of this study .....	5
<b>2 Material and Methods</b> .....	7
2.1 Bacterial strains and cultivation .....	7
2.1.1 Bacterial strains .....	7
2.1.2 Cultivation media .....	7
2.1.3 Sampling and cultivation .....	9
2.2 Microbiology methods .....	10
2.2.1 Determination of cell density .....	10
2.2.2 Preparing glycerol stock cultures .....	10
2.3 Molecular methods .....	10
2.3.1 Agarose gel electrophoresis .....	10
2.3.2 DNA extraction from liquid samples .....	11

2.3.3 RNA extraction from biofilms .....	12
2.3.4 Amplification of 16S rRNA gene .....	13
2.4 Sequencing, de novo assembly, and binning .....	14
2.4.1 Metagenome sequencing, processing, and analysis .....	14
2.4.2 RNA sequencing, processing, and analysis .....	15
2.4.3 Mass spectrometry and processing of secretome .....	15
2.5 Microscopy analyses .....	16
2.5.1 Fluorescence microscopy .....	16
2.6 Activity assays .....	17
2.6.1 Biofilm prevention assay .....	17
2.6.2 Biofilm degradation assay .....	17
2.7 Protein purification and processing .....	18
2.7.1 Fractionation of the supernatant via FPLC .....	18
2.7.2 SDS polyacrylamid gelelectrophoresis (SDS-PAGE) .....	18
2.8 Bioinformatics .....	20
2.8.1 Bioinformatics tools and databases.....	20
<b>3 Results</b> .....	21
3.1 Preliminary Screening of marine enrichment cultures .....	21
3.2 Comparison of biofilm production of two microorganisms .....	22
3.3 Microscopy and quantitative analyses of <i>Stenotrophomonas maltophilia</i> biofilm after treatment with different supplements .....	24
3.4 Metagenome-based microbial community analyses .....	26
3.5 Transcriptome analysis of <i>Stenotrophomonas maltophilia</i> biofilm after treatment with different supernatants .....	33
3.6 Secretome-based analysis of <i>M. foliosa</i> enrichment culture .....	39
3.7 Phylogenetic assignment and structural analysis.....	44
<b>4 Discussion</b> .....	47
4.1 Discovering anti-biofilm enzymes from marine enrichment cultures.....	47

4.2 Deep transcriptome analysis of <i>S. maltophilia</i> biofilm after stress induction ...	48
4.3 Biofilm degrading enzymes .....	49
4.4 Metalloproteases as promising anti-biofilm agents .....	50
4.5 Conclusion and outlook.....	52
<b>5 References</b> .....	<b>53</b>
<b>6 Acknowledgments</b> .....	<b>66</b>

## List of Figures

Figure 1: Schematic workflow of this study.....	6
Figure 2: Biofilm prevention and degradation assay with <i>Stenotrophomonas maltophilia</i> K279a treated with supernatants of different enrichment cultures .....	21
Figure 3: Biofilm prevention and degradation assay with <i>Stenotrophomonas maltophilia</i> K279a and <i>Pseudomonas aeruginosa</i> PA14 treated with supernatants of different enrichment cultures. ....	23
Figure 4: Confocal microscopic analysis of <i>Stenotrophomonas maltophilia</i> K279a biofilms .....	25
Figure 5: Analysis of the confocal microscopic images of <i>Stenotrophomonas maltophilia</i> biofilms .....	26
Figure 6: Phylogenetic analysis of microbial communities from an enrichment culture with <i>M. foliosa</i> .....	28
Figure 7: Phylogenetic analysis of microbial communities from an enrichment culture with water from a shark tank.....	29
Figure 8: Transcriptome analysis/ Circular genome mapping of <i>Stenotrophomonas maltophilia</i> K279a after treatment with supernatant of <i>M. foliosa</i> enrichment culture (GenBank: AM743169.1).....	34
Figure 9: Transcriptome analysis/ Circular genome mapping of <i>Stenotrophomonas maltophilia</i> K279a after treatment with supernatant of STW enrichment culture (GenBank: AM743169.1).....	35
Figure 10: Differentially expressed genes (DEGs) in <i>Stenotrophomonas maltophilia</i> K279a in response to <i>M. foliosa</i> enrichment culture .....	37
Figure 11: SDS-Page with fractions of the <i>M. foliosa</i> culture after fractionation with the FPLC system.....	41
Figure 12: Chromatogram of the <i>Montipora foliosa</i> culture after fractionation with the FPLC system and a Superdex® 200 10/300 GL gel filtration column.....	42
Figure 13: Structure prediction of microbial metalloprotease found in the proteome of the enrichment culture supernatant with <i>M. foliosa</i> .....	44
Figure 14: Phylogenetic tree of bacterial extracellular metalloproteases (BEMPS) grouped in MEROPS families .....	45
Figure 15: Schematic model of <i>S. maltophilia</i> biofilm including compounds, and proposed mechanism of metalloproteases .....	51



## List of Tables

Table 1: Bacterial strains and sources.....	7
Table 2: Samples from the Tropical Aquarium.....	9
Table 3: PCR program for 16S rRNA gene amplification.....	13
Table 4: Pipetting scheme for separating and stacking gel.....	19
Table 5: Bioinformatics tools.....	20
Table 6: Overall numbers of sequences and contigs generated for metagenome analysis of microbial communities from <i>Montipora foliosa</i> and from a shark tank ....	27
Table 7: Key features observed in the microbial communities from <i>Montipora foliosa</i> and a shark tank using IMG data analysis.....	30
Table 8: Key features of putative antimicrobial and Quorum quenching active enzymes. ....	32
Table 9: Overall numbers of sequences and contigs generated for the transcriptome datasets of <i>Stenotrophomonas maltophilia</i> K279a biofilm .....	33
Table 10: Heatmap of expression levels of differentially expressed genes response of <i>Stenotrophomonas maltophilia</i> K279a to <i>Montipora foliosa</i> enrichment culture.. ....	36
Table 11: Detected peptides in the supernatant of the enrichment culture with <i>M. foliosa</i> .....	40
Table 12: Most abundant proteins in the active fractions 23 and 24 of the enrichment culture supernatant with <i>Montipora foliosa</i> . ....	43

## List of Abbreviations

AHL	acyl-homoserine lactone
AMP	antimicrobial peptide
APS	ammonium persulfate
BMB	Bacto Marine Broth
BSA	bovine serum albumin
bidist.	double distilled
°C	degree Celsius
CLSM	confocal laser scanning microscopy
Da	Dalton
DNA	deoxyribonucleic acid
DMSO	dimethyl sulfoxide
DSF	diffusible signal factor
EDTA	ethylenediaminetetraacetic acid
e.g.	exempli gratia (“for example”)
EPS	extracellular polymeric substances
et al.	et alii (“and others”)
EtOH	ethanol
FPLC	fast protein liquid chromatography
g	gram
h	hour
IMG	Integrated Microbial Genomes and Microbiomes
k	kilo ( $10^3$ )
L	liter
LB	Lysogenic Broth
LC-MS	liquid chromatography - mass spectrometry
M	Molar
m	milli ( $10^{-3}$ )
min	minute
mol	mole

n	nano ( $10^{-9}$ )
NCBI	National Center for Biotechnology Information
NGS	Next Generation Sequencing
OD	optical density
PAGE	polyacrylamide gel electrophoresis
PCR	polymerase chain reaction
pH	potential of hydrogen
RNA	ribonucleic acid
SDS	sodium dodecyl sulfate
sec	seconds
T	temperature
TEMED	tetramethyl ethylenediamine
Tris	Tris(hydroxymethyl)aminomethane
UV	ultra-violet
v	volume
$\mu$	micro ( $10^{-6}$ )

## Abstract

Microbial biofilms are unwanted assemblages in clinics and industries. Once established biofilms are difficult to treat and to remove and different approaches have been developed to address this problem.

In this study, the focus was on the identification of novel anti-biofilm enzymes originating from the marine environment. To reach this target, enrichment cultures with five different coral species and water samples from a shark tank were prepared and supernatants were tested for their antibiofilm effects.

The supernatant of enrichment cultures with the stony coral *Montipora foliosa* and with water from a shark tank (STW22) showed a clear and reproducible reduction of biofilms of the gram-negative pathogenic bacterium *Stenotrophomonas maltophilia* K279a by about 40 %. Confocal laser scanning microscopy and other test confirmed these findings. To further identify the responsible proteins, a metagenomic analysis of the microbial communities of the enrichment cultures was performed. This study led to the discovery of 83,679,656 for the *M. foliosa* and 87,355,173 total sequences for the STW22 sample. The metagenomes coded for 47,903 and 85,886 genes and proteins, respectively. In the data sets, a total of 2,643 and 4,858 potential antimicrobial enzymes were discovered for the *M. foliosa* and the STW22 samples, respectively. In the next step, the transcriptome of K279a biofilm grown cells was analyzed estimate the effect of the supernatants on biofilm growth. A clear stress response of the bacterial pathogen in response to the supernatants was observed. Many genes linked to metal resistance, antitoxins, transporter, and iron acquisition were strongly up-regulated indicating that the supernatants had profound effects on the metabolism of the bacterial pathogen. Further investigations of the supernatants via fast protein liquid chromatography (FPLC) technique identified a group of 338 potential hydrolases having impact on the bacterial pathogen. The specific analysis of two fractions and alignments with databases led to ColA a *Bacillus cereus* metalloprotease belonging to the MEROPS family M9. In biofilm prevention assays with K279a reduction of the biofilm density by these fractions was confirmed.

In summary, enrichment cultures with marine material provided bioactive enzymes with strong antibiofilm activity. With the combination of metagenomic, transcriptomic, and proteomic approaches, a deep analysis of environmental samples and their effects on

other pathogenic bacterial strains was successful. A foundation could be created for further investigations on anti-biofilm enzymes.

## Zusammenfassung

Mikrobielle Biofilme sind unerwünschte Ansammlungen in Kliniken und Industrie. Einmal etablierte Biofilme sind schwer zu behandeln und zu entfernen, und es wurden verschiedene Ansätze zur Lösung dieses Problems entwickelt.

In dieser Studie lag der Schwerpunkt auf der Identifizierung neuartiger Anti-Biofilm-Enzyme, die aus der marinen Umgebung stammen. Um dieses Ziel zu erreichen, wurden Anreicherungskulturen mit fünf verschiedenen Korallenarten und Wasserproben aus einem Haifischbecken hergestellt und die Überstände auf ihre Anti-Biofilm-Wirkung getestet.

Der Überstand von Anreicherungskulturen mit der Steinkoralle *Montipora foliosa* und mit Wasser aus einem Haifischbecken (STW22) zeigte eine deutliche und reproduzierbare Reduzierung von Biofilmen des gramnegativen pathogenen Bakteriums *Stenotrophomonas maltophilia* K279a um etwa 40 %. Konfokale Laser-Scanning-Mikroskopie und andere Tests bestätigten diese Ergebnisse. Um die verantwortlichen Proteine weiter zu identifizieren, wurde eine metagenomische Analyse der mikrobiellen Gemeinschaften der Anreicherungskulturen durchgeführt. Diese Studie führte zur Detektion von 83.679.656 Sequenzen für die *M. foliosa* und 87.355.173 Sequenzen für die STW22-Probe. Die Metagenome kodierten für 47.903 bzw. 85.886 Gene und Proteine. In den Datensätzen wurden insgesamt 2.643 und 4.858 potenzielle antimikrobielle Enzyme für die *M. foliosa*- bzw. STW22-Proben entdeckt. Im nächsten Schritt wurde das Transkriptom von K279a-Biofilmzellen analysiert, um die Auswirkungen des Überstandes auf das Biofilmwachstum abzuschätzen. Als Reaktion auf die Überstände wurde eine deutliche Stressreaktion des bakteriellen Erregers beobachtet. Viele Gene, die mit Metallresistenz, Antitoxinen, Transportern und dem Eisenerwerb in Verbindung stehen, wurden stark hochreguliert, was darauf hindeutet, dass die Überstände tiefgreifende Auswirkungen auf den Stoffwechsel des bakteriellen Erregers hatten. Weitere Untersuchungen der Überstände mittels FPLC-Technik ergaben eine Gruppe von 338 potenziellen Hydrolasen, die Auswirkungen auf den bakteriellen Erreger haben. Die spezifische Analyse von zwei Fraktionen und der Abgleich mit Datenbanken führte zu ColA, einer Metalloprotease von *Bacillus cereus*, die zur MEROPS-Familie M9 gehört. In Biofilm-Präventionstests mit K279a wurde die Reduzierung der Biofilmdichte durch diese Fraktionen bestätigt.

Zusammenfassend lässt sich sagen, dass Anreicherungskulturen mit marinem Material bioaktive Enzyme mit starker Anti-Biofilm-Aktivität liefern. Mit der Kombination von metagenomischen, transkriptomischen und proteomischen Ansätzen gelang eine tiefgehende Analyse von Umweltproben und deren Auswirkungen auf andere pathogene Bakterienstämme. Damit konnte eine Grundlage für weitere Untersuchungen zu Anti-Biofilm-Enzymen geschaffen werden.

# 1 Introduction

## 1.1 Marine habitats as promising resources for bioactive molecules

Marine ecosystems offer huge biodiversity and plenty of new research approaches (Bayona et al., 2022, Cragg and Newman, 2005). Organisms like jellyfish, sponges, and corals live in environments with harsh conditions e.g., high temperatures, low pH values, and high pressure (Lordan et al., 2011, Giordano et al., 2021). They are also exposed to other species that compete with them for space and resources (Conte et al., 2020, Firm and Jones, 2000). Microorganisms living in symbiosis with these organisms produce a high diversity of bioactive molecules that can create an advantage in this competitive environment (König et al., 2006, Lopanik et al., 2004). These include compounds with unique characteristics, e.g., proteins, polysaccharides, and antioxidants (Lordan et al., 2011, Giordano et al., 2021).

In the last few years, the problem of multi-drug-resistant organisms has intensified. The research focuses on new substances with biological origins to handle bacterial infections. There is evidence of antibacterial, antifungal, and antiviral activity within the phylum of Actinobacteria (Prashith Kekuda et al., 2010, Manivasagan et al., 2013). About 42 % of all microbial secondary metabolites are produced by Actinobacteria (Prashith Kekuda et al., 2010, Lazzarini et al., 2000). Especially *Streptomyces* living in the marine environment are known for synthesizing antibiotics like Essramycin or Caboxamycin (Manivasagan et al., 2013, El-Gendy et al., 2008, Hohmann et al., 2009). Bioactive compounds originating from *Bacillus* strains which are settled in deep sea show antimicrobial, antifungal, and anticancer characteristics as well (Xiao et al., 2022, Subramenium et al., 2018). Cyclic lipopeptides, polyketides, and macrolactins were investigated for their promising antibacterial activity (Chen et al., 2017, Chakraborty et al., 2014, Chakraborty et al., 2017).

Microorganisms living in the skeleton and the mucus of corals are amongst others, substantial for the healthiness of these marine inhabitants (Chen et al., 2012, Chiou et al., 2010). They are supposed to synthesize potentially anti-microbial substances against pathogenic bacteria. Actinomycetes originating from corals are able to inhibit *Streptococcus pyogenes* biofilm formation (Chen et al., 2012, Nithyanand et al., 2010). Members of the phylum Firmicutes produce peptides that are beneficial for marine organisms and can be applied in industrial and medical areas (Vilela et al., 2021).



## **1.2 Metagenomics as a tool for enzyme discovery**

Metagenomics enables a deep view of the genomes of different microorganisms. Therefore, after taking an environmental sample, the DNA can be isolated either directly from the material or from enrichment cultures in specific media (Alma´abadi et al., 2015, Popovic et al., 2015). This technique increases the likelihood of finding a wider range of extraordinary putative antimicrobial agents in comparison to the cultivation of limited numbers of bacterial strains.

There are two basic approaches to identify interesting enzymes: function-based and sequence-based screenings (Simon and Daniel, 2011, Ferrer et al., 2008). The preparation of a genomic library and metabolic activity tests of single clones are principles of the function-based strategy (Simon and Daniel, 2011, Streit and Schmitz, 2004). The sequence-based analysis starts with the sequencing of metagenomic DNA and is followed by the screening for bioactive compounds via different bioinformatic tools and databases (Streit and Schmitz, 2004, Alma´abadi et al., 2015). Therefore, conserved domains of the genes coding for enzymes of interest need to be known (Alma´abadi et al., 2015).

## **1.3 Secondary metabolites with medical applications**

There is a series of secondary metabolites that is of high interest to the medical sector because of their antimicrobial characteristics. Classes like alkaloids, flavonoids, peptides, polyketides, fatty acids, and phenolic compounds can be found in algae, bacteria, and fungi (Kurhekar et al., 2020, Venkateskumar et al., 2020). Especially so-called AMPs (antimicrobial peptides) came into focus recently as promising medication (Mahlapuu et al., 2016, Bin Hafeez 2021). Several studies provided evidence of the antimicrobial activity of AMPs against bacteria, viruses, and fungi (Kang et al., 2017, Bin Hafeez et al., 2021). Furthermore, they are able to influence the innate immune system by improving wound healing or regulating the apoptosis of different immune cells (Fjell et al., 2012, Hancock and Sahl 2006).

Beyond that, glycosidases, proteases, and DNases are promising candidates for the inhibition or prevention of bacterial biofilms. Among other attacking points, they can degrade extracellular polymeric substances (EPS), and thereby increase the

permeability and vulnerability of biofilms for antibiofilm agents (Saggu et al., 2019, Algburi et al., 2017, Fleming and Rumbaugh 2017). Dispersin B is a glycoside hydrolase produced by *Actinobacillus actinomycetemcomitans* which can disrupt the polysaccharides in the biofilm of *Staphylococcus aureus* (Lister and Horswill 2014, Kaplan et al., 2004). Proteases are capable of disintegrating proteins, which are the critical components of the extracellular matrix (Saggu et al., 2019, Lister and Horswill 2014). Aureolysin (Aur), Staphopain A (ScpA), and Staphopain B (ScpB) are examples of proteases that are active on a mature *Staphylococcus aureus* biofilm (Fleming and Rumbaugh 2017, Lister and Horswill 2014). Another point of action represents the extracellular DNA which is important for the first phase of biofilm formation (Baslé et al., 2017, Whitchurch et al., 2002, Steinberger and Holden 2005). *Bacillus subtilis* and *Bacillus licheniformis* produce NucB, an enzyme that shows degradation activity in single and mixed-species biofilms (Baslé et al., 2017, Rostami et al., 2017).

#### **1.4 Microbial biofilms**

Microbial biofilms can be found on nearly every surface in flowing waters. Biofilms are an accumulation of one or more species in a self-produced polymeric matrix on biotic or abiotic surfaces (Høiby et al., 2011, Flemming et al., 2016). The matrix is built up of proteins, lipids, polysaccharides, and extracellular DNA (Hoiby et al., 2011, Flemming et al., 2022). The formation of such films is driven by quorum sensing mechanisms with the involvement of signal molecules like acyl-homoserine lactone (AHL) or a diffusible signal factor (DSF) (Huedo et al., 2018). With this machinery, the bacteria can synchronize the gene expression for cooperative behaviors. (Guendouze et al., 2017, AboZahra et al., 2013). After the first step of attachment on a surface of a few cells (i), follows sessile growth (ii), colonization and maturation (iii). The detachment and dispersal of cells (iv) complete the cycle of biofilm formation (Kumar et al, 2017, Tolker-Nielsen et al., 2015). The extracellular polymeric substances (EPS) serve as barriers against outer influences like antibiotics, predators, and chemicals (Flemming et al., 2016). It is also known that bacteria in such a clustering are protected against UV, metal toxicity, and pH gradients and are severalfold more resistant to antimicrobial agents than free-living microbes (Mishra et al., 2020, Padmavathi et al., 2014). Biofilm formation is often linked with bacterial infections in eukaryotic organisms. Several studies prove that about 80 % of all microbial infections in humans are caused by

biofilm-producing bacteria (Sharma et al., 2019, Fleming and Rumbaugh 2017, Römling and Balsalobre 2012). Especially devices, like artificial joints, catheters, and heart valves are susceptible to bacteria accumulation and thus to biofilm formation (Jamal et al., 2018, Darouiche et al., 2004, Zhang et al., 2021). In EPS microorganisms are in a starvation state and difficult to attack (Kumar et al., 2017, Cacaci et al., 2019). *Pseudomonas aeruginosa* and *Staphylococcus aureus* are the most common biofilm producers, which are well-studied (Guendouze et al., 2017, Driscoll et al., 2007, Lister and Horswill 2014). *P. aeruginosa* is known for its involvement in cystic fibrosis by forming microcolonies in the lung of patients (Algburi et al., 2017, Mulcahy et al., 2014, Singh et al., 2000). This infection can lead to reduced lung function and even to a fatal outcome (Diggle and Whiteley 2020, Elborn 2016). Besides, this pathogen was found in chronic wounds and on various medical devices (Mulcahy et al., 2014). *Staphylococcus aureus* colonizes mainly human nares and skin lesions and is also responsible for serious infections (Kwiecinski and Horswill, 2020, Wertheim et al., 2005). Once this pathogen enters the bloodstream it can cause sepsis and increase the susceptibility of the organism to further infections (Kwiecinski and Horswill, 2020, Angus et al., 2013). Both bacterial strains are highly resistant to most of the antibiotics used for diseases described above. *P. aeruginosa* shows resilience against aminoglycosides and  $\beta$ -lactams (Pang et al., 2018, Hancock and Speert 2000). In the last decades, methicillin-resistant *Staphylococcus aureus* (MRSA) became a threat to every hospital and forced researchers to look intensively for new alternatives (Guo et al., 2020, Lakhundi and Zhang 2018).

### **1.5 Potential pathogenic bacterium *Stenotrophomonas maltophilia***

Another biofilm former has been getting attention recently: *Stenotrophomonas maltophilia*. This bacterium is aerobic, Gram-negative, rod-shaped, and belongs to the Gammaproteobacteria (Hansen et al., 2012, Alio et al., 2020). It has come into focus because of its potential pathogenicity and important role in human infections like pneumonia, bacteremia, and endocarditis (Sánchez et al., 2015, Brooke 2012, Abda et al., 2015). This nosocomial organism forms thick biofilms in the lungs of immunocompromised patients and on medical devices as well. The control of infections with this microorganism is quite challenging because of its high resistance against most of the applied antibiotics, like cephalosporins, tetracyclines, and  $\beta$ -lactam

antibiotics (Abda et al., 2015, Brooke 2012). This resilience is, among other things, attributed to efflux pumps, modifying enzymes,  $\beta$ -lactamases, and low permeability of the outer membrane (Crossman et al., 2008, Looney et al., 2009, Brooke et al., 2017). The quorum sensing molecules (DSFs), which are important for cell-to-cell signaling and thus for biofilm formation in *S. maltophilia*, play a role in controlling antibiotic resistance as well (Crossman et al., 2008, Barber et al., 1997).

## **1.6 Aim of this study**

In this study, new biomolecules with anti-microbial activity from marine habitats should be identified and characterized. Therefore, enrichment cultures with marine material were used as a starting point, followed by biofilm plate assays to narrow it down to a few cultures. Sequence-based screenings of the isolated genomic DNA, combined with metagenomics, were used for the identification of promising candidates. Furthermore, deep analysis with confocal microscopy and activity tests proved the effectiveness of the samples. Finally, protein fractionation and purification led to the identification of key enzymes.

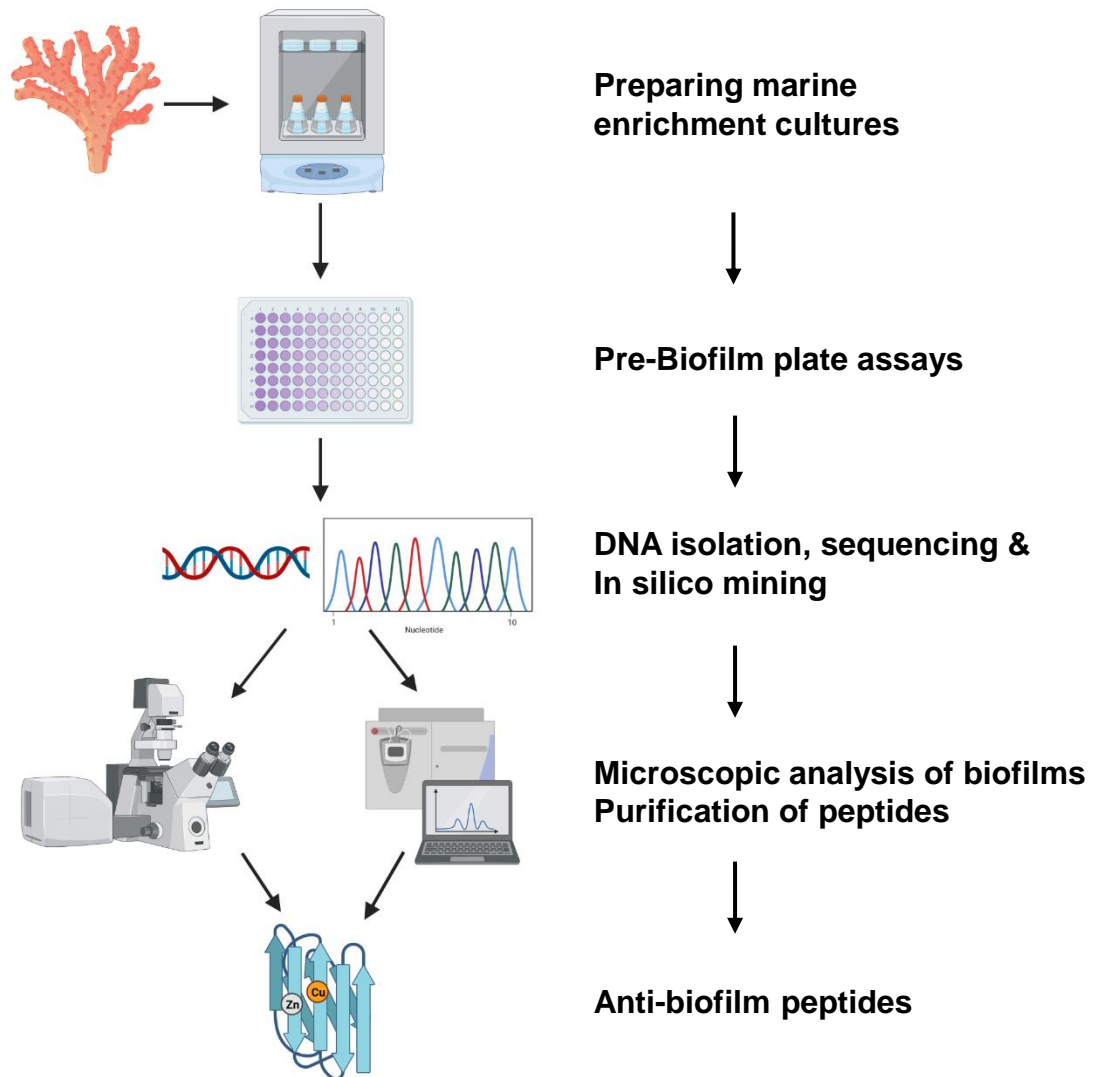


**Figure 1: Schematic workflow of this study.** Enrichment cultures were prepared with marine samples and the supernatant was used for biofilm plate assays. After isolation and sequencing of the genomic DNA, the dataset was screened for interesting candidates. With confocal microscopy, the treated biofilm of *S. maltophilia* was investigated and FPLC was used for the fractionation and purification of putative anti-biofilm peptides. Created with BioRender.com.

The focus of this research project was on proteins attacking and thus preventing biofilms from bacterial strains, like *S. maltophilia* and *P. aeruginosa*. These microorganisms represent a serious threat to the medical sector and are getting attention for causing infections with high antibiotic resistance.

On the one hand, this study was important for understanding biofilm formation and the stress response of pathogenic organisms, and on the other hand for the identification of attack points in biofilm structures.

## 2 Material and Methods

### 2.1 Bacterial strains and cultivation

#### 2.1.1 Bacterial strains

All bacterial strains used in this study are listed in the table below (Table 1).

**Table 1: Bacterial strains and characteristics.**

<b>Strain</b>	<b>Characteristics</b>
<i>Stenotrophomonas maltophilia</i> K279a	Gram-negative, rod-shaped, obligate aerobic, non-fermentative, $\beta$ -lactam antibiotic resistance (Hansen 2012, Abda et al., 2015)
<i>Pseudomonas aeruginosa</i> PA14	Gram-negative, rod-shaped, aerobic–facultatively anaerobic, high virulence (Sharma et al., 2013, Grace et al., 2022)

The bacterial strains (Table 1) were cultivated in liquid LB medium at 37 °C overnight under constant shaking.

#### 2.1.2 Cultivation media

All media were autoclaved at 121 °C and 2 bar for 20 min before use. Antibiotics and heat-sensitive additives were filtered sterilely and added after cooling the medium to a temperature of 55-60 °C.

Bacto Marine Broth (Difco 2216, modified by M. Peters)

Bacto peptone	5 g
Bacto yeast extract	1 g
Fe(III) citrate	0.1 g
NaCl	19.45 g
MgCl <sub>2</sub> (anhydrous)	12.40 g
Na <sub>2</sub> SO <sub>4</sub>	3.24 g
CaCl <sub>2</sub>	1.80 g
KCl	0.55 g
NaHCO <sub>3</sub>	0.16 g
KBr	0.08 g
SrCl <sub>2</sub>	0.0559 g
H <sub>3</sub> BO <sub>3</sub>	0.022 g
Na-selicate	0.004 g
NaF	0.0024 g
(NH <sub>4</sub> ) NO <sub>3</sub>	0.0016 g
Na <sub>2</sub> HPO <sub>4</sub>	0.008 g
Distilled water	ad 1000 mL

The pH value was adjusted to 7.6.

Lysogeny Broth (LB) medium (Bertani, 1951)

Tryptone/ peptone	10 g
Yeast extract	5 g
NaCl	5 g
Distilled water	ad 1000 mL

The pH value was adjusted to 7.0.

### 2.1.3 Sampling and cultivation

Samples of five coral species and 2 L of water from the shark tank were taken at the Hagenbeck Tropical Aquarium (Lokstedter Grenzstraße 2, 22527 Hamburg, Germany). The stony corals *Montipora foliosa*, *Montipora hodgsoni*, *Seriatopora caliendrum*, *Acropora* sp., and the soft coral *Sinularia brassica* were collected (Table 2).

**Table 2: Samples from the Tropical Aquarium.**

<b>Species/ Sample type</b>	<b>Sampling conditions</b>
<i>Montipora foliosa</i>	26 °C, pH 8.0
<i>Montipora hodgsoni</i>	26 °C, pH 8.0
<i>Seriatopora caliendrum</i>	26 °C, pH 8.0
<i>Acropora</i> sp.	26 °C, pH 8.0
<i>Sinularia brassica</i>	26 °C, pH 8.0
Shark tank water	22 – 25 °C, pH 8.0

For the cultivation, a modified Bacto Marine Broth (DIFCO 2216) was used (section 2.1.2). The corals were broken into smaller pieces and 0.5 g of each species was used for enrichment cultures in 50 mL Bacto Marine Broth which was inoculated at 28 °C under constant shaking. In addition, 0.5 mL of the water sample was used for cultures in the same medium with incubation temperatures at 22 °C, 28 °C, and 37 °C. After three days all cultures were centrifuged for 20 min at 4 °C and 5.000 x g. The supernatant was filtered twice through a 0.2 µm syringe filter (ClearLine, Kisker Biotech GmbH & Co.KG, Steinfurt, Germany).



## **2.2 Microbiology methods**

### **2.2.1 Determination of cell density**

The cell density of liquid cultures was determined photometrically in semi-micro disposable cuvettes with a layer thickness of 10 mm (Ratiolab GmbH, Dreieich-Buschlag, Germany). The measurement was performed using an absorption single-beam photometer at a wavelength of  $\lambda = 600$  nm (OD600). The adequate volume of the medium acted as a standard before each measurement. For calculation of the cell density of a solution, it is assumed that an OD600 of 0.1 correlates to a cell concentration of  $1 \times 10^8$  *E. coli* cells/ mL.

### **2.2.2 Preparing glycerol stock cultures**

For glycerol stock cultures, 600  $\mu$ L of a fresh, overnight-grown culture was mixed with 600  $\mu$ L of sterile 86 % glycerol and stored in a reaction vessel with a screw cap at -70 °C.

## **2.3 Molecular methods**

For sterilization and inactivation of nucleases, heat-stable devices, and solutions were autoclaved at 121 °C for 20 min. Non-heat-stable devices were rinsed with 70 % ethanol and the required solutions were sterile filtered.

### **2.3.1 Agarose gel electrophoresis**

With the technique of agarose gel electrophoresis, it is possible to separate nucleic acids from different sources (PCR, DNA, and RNA isolation) according to size. The samples were mixed with DNA Gel Loading Dye (Thermo Scientific Scientific, Waltham, MA, USA) and loaded onto the gel. For direct comparison, a DNA ladder (Thermo Scientific Scientific, Waltham, MA, USA) moderate for the size range was also applied. A voltage source was connected to the chamber. Unless otherwise noted, 0.8 % agarose gels were run at 100 volts for 30 minutes. The gel was then incubated in

an ethidium bromide bath (10 µg/mL) for 12 minutes and subsequently monitored under UV light.

#### TAE-buffer (10x)

Tris	0.4 M
EDTA x Na <sub>2</sub> x 2H <sub>2</sub> O	0.01 M

The pH value was adjusted to 8.2 with acetic acid.

### **2.3.2 DNA extraction from liquid samples**

The first activity test (section 2.6.1) with the supernatant of the six enrichment cultures narrowed it down to two samples. After three days of incubation, 4 mL of the enrichment culture with the coral *Montipora foliosa* and with water from the shark tank (STW22), was centrifuged for 15 min at 4 °C and 5.000 x g. The DNA of each cell pellet was isolated with the NucleoSpin Microbial DNA Kit (Machery-Nagel, Düren, Germany) and the protocol was followed. The nucleic acid concentration and purity of the DNA samples were measured with a Nano Photometer (Implen NanoPhotometer, ThermoFisher Scientific, Waltham, MA, USA).

### 2.3.3 RNA extraction from biofilms

*Stenotrophomonas maltophilia* K279a was grown in liquid LB medium overnight and diluted with the appropriate medium up to  $OD_{600\text{ nm}} = 0.05$ . An amount of 500  $\mu\text{L}$  *S. maltophilia* culture was added to 24-well microtiter plates with Nunclon delta surface (Thermo Fisher Scientific, Waltham, MA) and treated with 500  $\mu\text{L}$  of supernatant of the enrichment cultures with *M. foliosa* and STW22. After incubation at 37 °C for 24 h, the RNA was isolated from the mature biofilm as described below. The procedure was fundamentally based on the TRIzol™ Reagent User Guide (Zymo Research, Irvine, United States). The biofilm cells were washed out with in total 1 mL TRIzol™ Reagent (Zymo Research, Irvine, United States) and centrifuged at a speed of 4500 x g for 20 min at 4 °C. To extract the RNA, the pellet was mixed with chloroform and incubated for 7 min at room temperature. It was followed by a centrifugation step at 12,000 x g and 4 °C for 12 min. The upper aqueous phase was agitated with 1 mL isopropyl alcohol, incubated for 7 min at room temperature, and centrifuged at 12,000 x g and 4 °C for 8 min. The nucleotides were precipitated by adding 2 mL of 70 % (v/v) EtOH to the supernatant and followed by centrifugation at 7500 x g and 4 °C for 5 min. The EtOH was removed, and the pellet was dried in a vacuum concentrator (SpeedVac, ThermoFisher Scientific, Waltham, MA) and resuspended in 90  $\mu\text{L}$  diethylpyrocarbonate (DEPC)-treated water. The DNA was removed with the DNase kit (RNase-free DNase set, Qiagen, Hilden, Germany). Afterwards, the sample was mixed with 200  $\mu\text{L}$  RNase-free water and 200  $\mu\text{L}$  PCI (50 % phenol/ 48 % chloroform/ 2 % isoamyl alcohol) and loaded on a Phase Lock reaction tube (5PRIME Phase Lock Gel, Quantabio, MA). After centrifugation at 11,000 x g for 10 min at 4 °C, the supernatant was transferred to a new reaction tube. The RNA was precipitated by adding 25  $\mu\text{L}$  3 M NaAc (pH 5.2) and 1 mL ice-cold 96 % (v/v) EtOH. The precipitation of the RNA took place overnight. The sample was centrifuged at 12,000 x g for 30 min at 4 °C, the supernatant was discarded, and the pellet was dried in the vacuum concentrator. Finally, the RNA was dissolved in 50  $\mu\text{L}$  DEPC-treated water and was stored at -70°C. The concentration and quality of the RNA were measured using a Nano Photometer (Implen NanoPhotometer, ThermoFisher Scientific, Waltham, MA) and verified on a 0.8 % agarose gel. Optionally another DNase treatment or a clean-up with the RNA Clean&Concentrator™ Kit (Zymo Research Europe, Freiburg, Germany) was performed.

### 2.3.4 Amplification of 16S rRNA gene

To verify the purity and the absence of any DNA in the RNA isolation samples, a PCR of the 16S rRNA gene was performed. The gene was amplified with the instructions described below and the PCR products were checked on a 0.8 % agarose gel.

#### 50 $\mu$ L-approach

Phusion polymerase (Thermo)	0.5 $\mu$ L
5 x GC-buffer (Thermo)	10 $\mu$ L
Forward primer: 616 V	2 $\mu$ L
Reverse primer: 1429 R	2 $\mu$ L
dNTPs (10 mM)	1 $\mu$ L
DMSO	1.5 $\mu$ L
RNA	1 $\mu$ L
Distilled water	ad 50 $\mu$ L

**Table 3: PCR program for 16S rRNA gene amplification.**

<b>Step</b>	<b>Temperature</b>	<b>Time</b>	
Initial denaturation	98 °C	10 min	
Denaturation	98 °C	30 sec	} 32x
Annealing	52 °C	30 sec	
Elongation	72 °C	1.5 min	
Final elongation	72 °C	5 min	

## 2.4 Sequencing, de novo assembly, and binning

### 2.4.1 Metagenome sequencing, processing, and analysis

DNA extracted from the enrichment culture with *M. foliosa* and with STW22 was used to perform metagenome analysis by Next-Generation sequencing at the Heinrich-Pette-Institute (HPI, Hamburg, Germany). Prior to library generation, the concentration of the extracted DNA samples was measured with the DNA High Sensitivity Assay Kit on a Qubit 2.0 (Thermo Fisher Scientific, Waltham, MA). DNA libraries were then generated using the NEBNext® Ultra™ DNA Library Prep Kit for Illumina® (New England Biolabs, Frankfurt am Main, Germany) according to the manufacturer's instructions. Concentrations of the generated libraries were measured with the DNA HS Assay Kit on a Qubit 2.0 (Thermo Fisher Scientific, Waltham, MA). Additionally, the mean fragment length of each library was determined with the DNA High Sensitivity Chip (Agilent Technologies, Inc., Santa Clara, USA) on an Agilent 2100 Bioanalyzer (Agilent Technologies). All samples were diluted to 2 nM and an equimolar pool was generated. Paired-end sequencing (2x150 bp) of the pool was performed on a NextSeq500 (Illumina, San Diego, USA) aiming for ~80 million reads per sample. Reads were mapped to a similar host genome: *Montipora efflorescens* (<https://www.ncbi.nlm.nih.gov/bioproject/509803>). For this purpose, bowtie2 (Langmead and Salzberg, 2012) version 2.3.5.1 was used, and unmapped reads were then extracted using SAMtools (Li et al., 2009) and assembled into scaffolds using SPAdes genome assembler (Prjibelski et al., 2020) version 3.10.1. Contigs obtained after *de novo* assembly of a length greater than 1kb were only selected for the analysis. Further analysis of the sequences was done with the help of the Integrated Microbial Genomes (IMG) system (Markowitz et al., 2012, <https://gold.jgi.doe.gov/>).

### 2.4.2 RNA sequencing, processing, and analysis

The samples were processed by Eurofins Genomics Europe Sequencing GmbH (Constance, Germany), where the RNA was assessed for QC. The RNA Integrity Number (RIN) for all samples was  $\geq 8$ . Strand-specific cDNA library preparation from polyA enriched RNA (150 bp mean read length) and RNA sequencing was performed using the genome sequencer Illumina HiSeq technology in NovaSeq 6000 S4 PE150 XP sequencing mode. For further analysis, fastq-files were provided.

RNA-seq analysis was performed using PATRIC, the Pathosystems Resource Integration Center ([www.patricbrc.org](http://www.patricbrc.org)). Trim Galore 0.6.5dev was used to remove adapters (Phred quality score below 20) (Krueger et al., 2012). RNA-Seq data was processed by the tuxedo strategy (Trapnell et al., 2012). All genes were selected with  $|\log_2(\text{fold change})| \geq 1,5$ . The differentially expressed genes (DEGs) dataset was collected and used for further analysis. The volcano plot of the distribution of all DEGs was generated using a Shiny app ggVolcanoR (Mullan et al., 2021).

### 2.4.3 Mass spectrometry and processing of secretome

The supernatant of the *M. foliosa* culture and a control with Bacto Marine Broth, were sent to NH DyeAGNOSTICS GmbH (Halle, Germany) for deep analysis of the proteome according to Goodman et al., 2018. In the first step, reduction and alkylation of the samples and a tryptic digest were performed. The measurement of tryptic peptides by electrospray ionization mass spectrometry coupled with liquid chromatography (nano-RP-HPLC-ESI-QTOF-MS/MS; Waters nano ACQUITY UPLC coupled with Waters Synapt G2-Si) followed. The acquired MS data were processed with Mascot Distiller software. Provided sequence data, Swiss-Prot/UniProt (universal protein database, <https://www.uniprot.org>, The UniProt Consortium 2021) and database of *Bacillus cereus* were used with different filters (trypsin, 2 missed cleavage sites, carbamidomethyl modification (Cys), and oxidation (Met)). Unassigned spectra were analyzed using Peaks software (BSI). The results were provided as filtered (filter: min. 3 detected peptides per protein), unfiltered, and de novo peptides (generated using Peaks; BSI).

The supernatant of the promising cultures was fractionated via FPLC (section 2.7.1) and selected fractions were sent to NH DyeAGNOSTICS GmbH for further MS-analysis and the results aligned with UniProt.

## **2.5 Microscopy analyses**

### **2.5.1 Fluorescence microscopy**

To examine the structure of the biofilm after treatment with the supernatants of the selected enrichment cultures, the confocal laser scanning microscope (CLSM, Carl Zeiss Microscopy GmbH, Jena, Germany) was used. The samples were prepared in 8-well  $\mu$ -slides (ibidi GmbH, Gräfelfing, Germany). In each well 100  $\mu$ L overnight culture of a biofilm former (diluted with the appropriate medium up to  $OD_{600\text{ nm}} = 0.05$ ) and 100  $\mu$ L of the prepared supernatants were added. After incubation of the slide at 37°C for 16 h, the cells were stained with the LIVE/DEAD BacLight bacterial viability kit (Thermo Fisher Scientific, Waltham, MA, USA). Images of the biofilm were taken according to Alio et al., 2020 at the CLSM Axio Observer.Z1/7 LSM 800 with airyscan (Carl Zeiss Microscopy GmbH, Jena, Germany) and a C-Apochromat 63x/1.20W Korr UV VisIR objective. In each case, the biofilm former plus the used medium acted as a control. At least three different spots in one sample were chosen for the images. All pictures were processed with ZEN system software (version 2.3; Carl Zeiss Microscopy GmbH). Afterwards, the images were analyzed quantitatively with the program BiofilmQ software version 0.1.4 (<https://drescherlab.org/data/biofilmQ/>, Hartmann et al., 2021). The number of living and dead cells and the biofilm thickness were subjected to a paired sample t-test and the p-value was assigned to determine if the two samples were significantly different from each other.

## **2.6 Activity assays**

### **2.6.1 Biofilm prevention assay**

To determine the biofilm density of model organisms after treatment with different supplements, a crystal violet assay was used. The protocol was based on Steinmann et al., 2018. Assays were performed in 96-well microtiter plates with Nunclon delta surface (Thermo Fisher Scientific, Waltham, MA, USA). An overnight culture of *Stenotrophomonas maltophilia* K279a or *Pseudomonas aeruginosa* PA14 was prepared and diluted after 24 h in LB medium up to  $OD_{600\text{ nm}} = 0.05$ . 100  $\mu\text{L}$  of the culture was pipetted into 6 wells and 100  $\mu\text{L}$  of each enrichment culture supernatant was added. After incubation at 37 °C for 24 h, the planktonic cells were removed, and the plate was dried at 65 °C for 60 min. In each well, 50  $\mu\text{L}$  of 0.5 % crystal violet was added and incubated for 5 min at room temperature. The microtiter plate was washed three times with water and tapped onto a paper towel. It was followed by a drying step at 37 °C for 30 min. After adding 150  $\mu\text{L}$  of 33 % acetic acid to each well, the amount of solubilized biofilm was measured at a plate reader and a wavelength of 595 nm. The biofilm density was determined and subjected to a paired sample t-test and the p-value was assigned to determine if the two samples were significantly different from each other.

### **2.6.2 Biofilm degradation assay**

The activity of the enrichment culture supernatants on mature biofilm was tested via degradation assay in 96-well plates (Thermo Fisher Scientific, Waltham, MA, USA). An overnight culture of the biofilm former was prepared and diluted after 24 h in LB medium up to  $OD_{600\text{ nm}} = 0.05$ . 100  $\mu\text{L}$  of the culture was pipetted into 6 wells of the plate and incubated for 24 h at 37 °C. An amount of 100  $\mu\text{L}$  of different supplements was added and another incubation step at 37 °C for 24 h followed. The further steps were the same as in the prevention assay.



## **2.7 Protein purification and processing**

### **2.7.1 Fractionation of the supernatant via FPLC**

Fast protein liquid chromatography (FPLC, Amersham Biosciences ÄKTA FPLC system, Marshall Scientific, Hampton NH) was used for further analysis of the supernatant. The enrichment cultures of *M. foliosa* and the shark tank were centrifuged at 5,000 x g for 20 min at 4 °C and the supernatants were filtered through a 0.2 µm syringe filter (ClearLine, Kisker Biotech GmbH & Co. KG, Steinfurt, Germany). Afterwards, the supernatants were concentrated in the vacuum centrifuge (SpeedVac, ThermoFisher Scientific, Waltham, MA) and filtered through a syringe filter again. The prepared samples were loaded on a Superdex® 200 10/300 GL gel filtration column (Sigma-Aldrich Chemie GmbH, Taufkirchen, Germany) with potassium phosphate buffer pH 7.0 as a moving fluid. The fractionation occurred in 1 mL steps with a flow rate of 0.75 mL/min and the UV spectrum was analyzed with the UNICORN™ system (<https://www.cytivalifesciences.com>, Gotesman et al., 2021) control software.

### **2.7.2 SDS polyacrylamid gelectrophoresis (SDS-PAGE)**

With the technique of SDS-PAGE, proteins can be separated according to size. The sodium dodecyl sulfate attaches itself to the molecule and a negative charge is formed over the entire protein. In the electric field, the proteins move from the cathode to the anode due to this charge. The polyacrylamide acts as a molecular sieve, allowing smaller proteins to move through the gel more quickly compared to larger ones. SDS-PAGE consists of two gels, the separating gel, and the stacking gel (Laemmli 1970, Schägger 2006) (Table 4).

After polymerization, the polyacrylamide gels were placed in a running chamber and a voltage source was connected. Next to the FPLC fraction samples, a protein ladder (PageRuler™ Unstained Protein Ladder, Thermo Fisher Scientific, Waltham, MA, USA) was applied and the gel was run for approximately one hour at 120 V. In the next step, the gels were stained with the Pierce™ Silver Stain Kit (Thermo Fisher Scientific, Waltham, MA, USA).

**Table 4: Pipetting scheme for separating and stacking gel.**

<b>Solution</b>	<b>12% separating gel</b>	<b>7% stacking gel</b>
Acrylamide stock solution	3.0 mL	0.7 mL
Separating gel stock solution	2.5 mL	-
Stacking gel stock solution	-	0.96 mL
H <sub>2</sub> O bidest	4.5 mL	2.34 mL
TEMED	9 µL	6 µL
APS	45 µL	20 µL

10x Electrophoresis buffer

Tris	30.3 g
Glycine	144.1 g
SDS	10 g
Distilled water	ad 1000 mL

The pH value was adjusted to 8.4.

Separating gel stock solution

Tris	6.1 g
SDS	0.4 g
Distilled water	ad 100 mL

The pH value was adjusted to 6.8.

Stacking gel stock solution

Tris	18.2 g
SDS	0.4 g
Distilled water	ad 100 mL

The pH value was adjusted to 8.8.

## 2.8 Bioinformatics

### 2.8.1 Bioinformatics tools and databases

Further bioinformatics tools used in this study for processing and analysis of metagenomic, transcriptomic, and proteomic datasets are listed in the table below (Table 5).

**Table 5: Bioinformatics tools.**

<b>Designation</b>	<b>Application</b>	<b>Source</b>
BLAST (n and p)	Protein and nucleotide sequence searches against NCBI's database	(Sayers et al., 2021)
IMG Gold	Annotation and analysis of genome datasets	(Markowitz et al., 2012)
Mega X (10.2.4)	Molecular evolutionary genetics analysis	(Kumar et al., 2018)
Robetta server	Protein structure prediction	(Park et al., 2018)
T-Coffee	Multiple sequence alignments	(Notredame et al., 2000)
UCSF ChimeraX (1.3)	Protein structure visualization	(Pettersen et al., 2021)
UniProt	Database of protein sequences and functions	(The UniProt Consortium 2021)

## 3 Results

### 3.1 Preliminary Screening of marine enrichment cultures

The enrichment cultures with material from the Tropical Aquarium were analyzed after an incubation of 3 days at 37 °C. All samples were centrifuged, and the sterile filtered (0.2 µm) supernatant was used for preliminary biofilm assays. An overnight culture of the model organism *Stenotrophomonas maltophilia* K279a was grown in 96-well plates and treated with sterile supernatants before or after the biofilm formation. The biofilm density was measured after 24 h and compared to a control treated with Bacto Marine Broth (BMB). Figure 2 showed the results of the biofilm prevention and degradation assay. The samples enriched with the stony coral *Montipora foliosa* and with water from the shark tank (STW) incubated at 22 °C significantly reduced the density by about 50%. Both samples demonstrated a degradation activity of up to 30 % in comparison to the control.

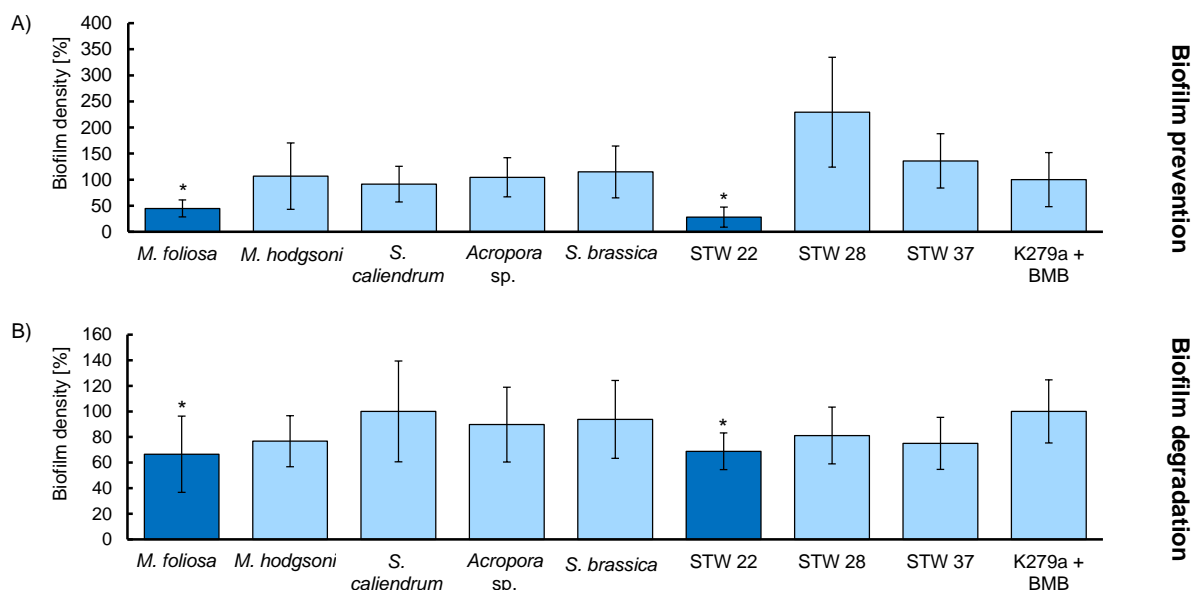


**Figure 2: Biofilm prevention and degradation assay with *Stenotrophomonas maltophilia* K279a treated with supernatants of different enrichment cultures.** The enrichment cultures were inoculated with parts of the following corals: *Montipora foliosa*, *Montipora hodgsoni*, *Seriatopora caliendrum*, *Acropora* sp., *Sinularia brassica*, and with water from a shark tank (STW) at different temperatures (22 °C, 28 °C, and 37 °C). The K279a culture was incubated with supernatants for 24 h (prevention (A)) or treated with supplements after biofilm formation (degradation (B)) in 96-well plates. The biofilm was stained with 0.5% crystal violet and the density was measured at a wavelength of 595 nm. All samples were compared with the negative control *S. maltophilia* (K279a) treated with Bacto Marine Broth (BMB). In the prevention assay, the sample with *M. foliosa* and STW22 significantly reduced the biofilm density with a p-value of  $1.3 \times 10^{-5}$  and  $1.3 \times 10^{-7}$ , respectively. The degradation assay showed a biofilm reduction for *M. foliosa* and STW22 with a p-value of  $3.3 \times 10^{-3}$  and  $2.2 \times 10^{-5}$ , respectively. The data are mean values of at least three replicates. The error bars indicate simple standard deviations (original figure from Peters et al., 2023, modified by M. Peters).

### **3.2 Comparison of biofilm production of two microorganisms**

Biofilm prevention and degradation assays with *Stenotrophomonas maltophilia* K279a and *Pseudomonas aeruginosa* PA14 were performed to test the anti-biofilm effect against two serious pathogenic organisms in direct comparison. K279a and PA14 cultures were either incubated directly with the supernatants for 24 h or treated after biofilm formation for 24 h in 96-well plates. The biofilm was stained with 0.5 % crystal violet and the density was measured at a wavelength of 595 nm. All samples were compared with the negative control K279a or PA14 incubated with Bacto Marine Broth (BMB) (Figure 3).

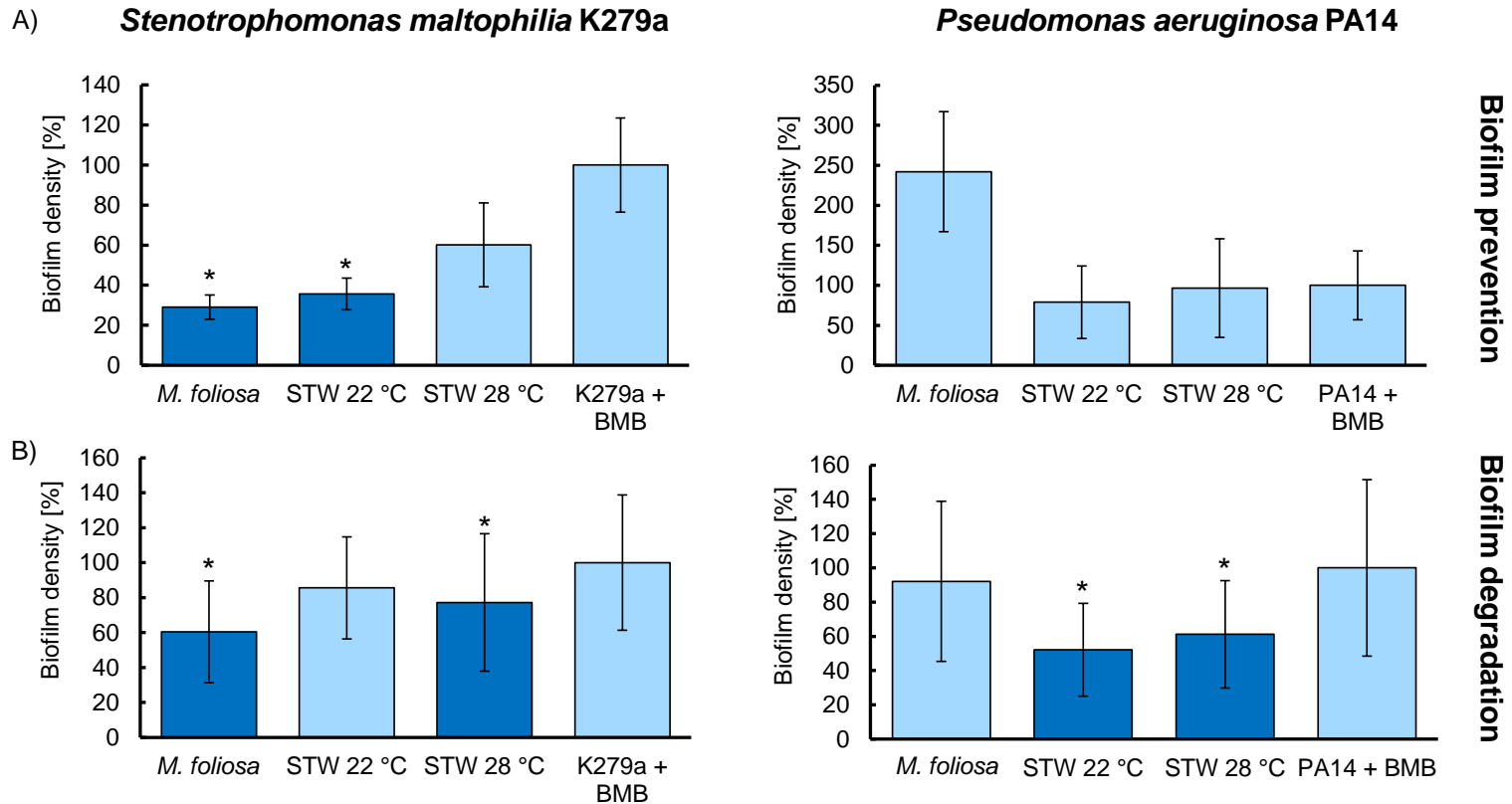


**Figure 3: Biofilm prevention and degradation assay with *Stenotrophomonas maltophilia* K279a and *Pseudomonas aeruginosa* PA14 treated with supernatants of different enrichment cultures.** The K279a and PA14 cultures were incubated with supernatants for 24 h (prevention (A)) or treated with supplements after biofilm formation (degradation (B)) in 96-well plates. The biofilm was stained with 0.5 % crystal violet and the density was measured at a wavelength of 595 nm. All samples were compared with the negative control K279a or PA14 treated with Bacto Marine Broth (BMB). In the prevention assay, the sample with *M. foliosa* and STW22 significantly reduced the biofilm density of K279a with a p-value of 0.011 and 0.014, respectively. The degradation assay showed a biofilm reduction of K279a for *M. foliosa* and STW28 with a p-value of 0.025 and  $1.2 \times 10^{-3}$ , respectively. In addition, significant degradation of PA14 biofilm was detected by sample STW22 with a p-value of  $4.0 \times 10^{-4}$  and by sample STW28 with a p-value of  $1.2 \times 10^{-3}$ . The data are mean values of at least three replicates. The error bars indicate simple standard deviations.

Interestingly, the enrichment culture supernatant with *M. foliosa* showed prevention and degradation activity against K279a but not against PA14. This sample significantly reduced the biofilm density of *S. maltophilia* up to 70 % and 40 % and with a p-value of 0.011 and 0.025, respectively. The enrichment culture with shark tank water (STW) incubated at 22 °C demonstrated slight prevention and strong degradation activity against *P. aeruginosa* and reduced the biofilm by about 20 % and 55 %, respectively. Additionally, this sample significantly prohibited the biofilm formation of *S. maltophilia* by about 65 % and a p-value of 0.014. The supernatant of the enrichment culture with shark tank water incubated at 28 °C convinced in the degradation of K279a and PA14 biofilm. It clearly reduced the density of both biofilms up to 40 %.

### **3.3 Microscopy and quantitative analyses of *Stenotrophomonas maltophilia* biofilm after treatment with different supplements**

The investigation of *S. maltophilia* K279a biofilm structure via confocal laser scanning microscopy provided detailed insight into the building and destruction of a biofilm. The biofilm former was grown in chamber slides and treated with the supernatants of the cultures enriched with *M. foliosa* and STW22. After the incubation for 16 h at 37 °C, the biofilm was stained with 0.5 % crystal violet and analyzed at CLSM. The images (Figure 4) illustrated a clear difference between the biofilm incubated with the supplements and the control. Both treated samples exhibited several holes and a porous structure in comparison to the strain grown with BMB.

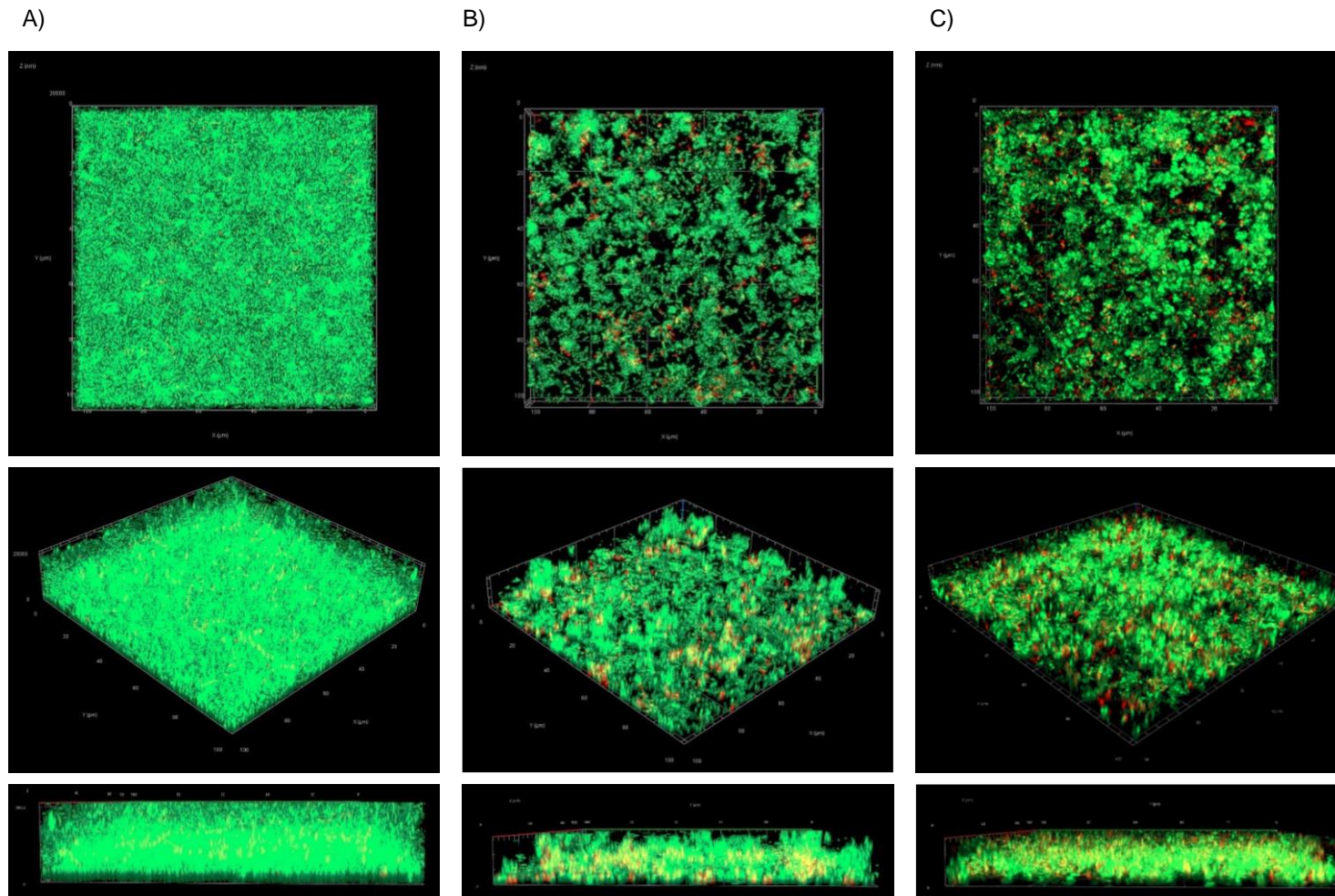


**Figure 4: Confocal microscopic analysis of *Stenotrophomonas maltophilia* K279a biofilms.** Structural analysis of (A) control: K279a + Bacto Marine Broth (BMB), (B) K279a + sterile filtered supernatant of an enrichment culture of *Montipora foliosa*, and (C) K279a + sterile filtered supernatant of an enrichment culture with water of a shark tank (STW). Cells were grown under static conditions for 16 h in LB medium and treated with different supplements. Stained with LIVE/DEAD staining, green: living cells, red: dead cells, and investigated with CLSM. Images represent an area of 100 µm by 100 µm of the biofilm (original figure from Peters et al., 2023, modified by M. Peters).



The total number of cells and the biofilm thickness were evaluated with BiofilmQ and presented in Figure 5. The control showed 34,961 cells: 26,139 living and 8,822 dead cells. In comparison, the investigation of the *M. foliosa* sample provided 16,457 living and 16,181 dead cells (Figure 5 A).

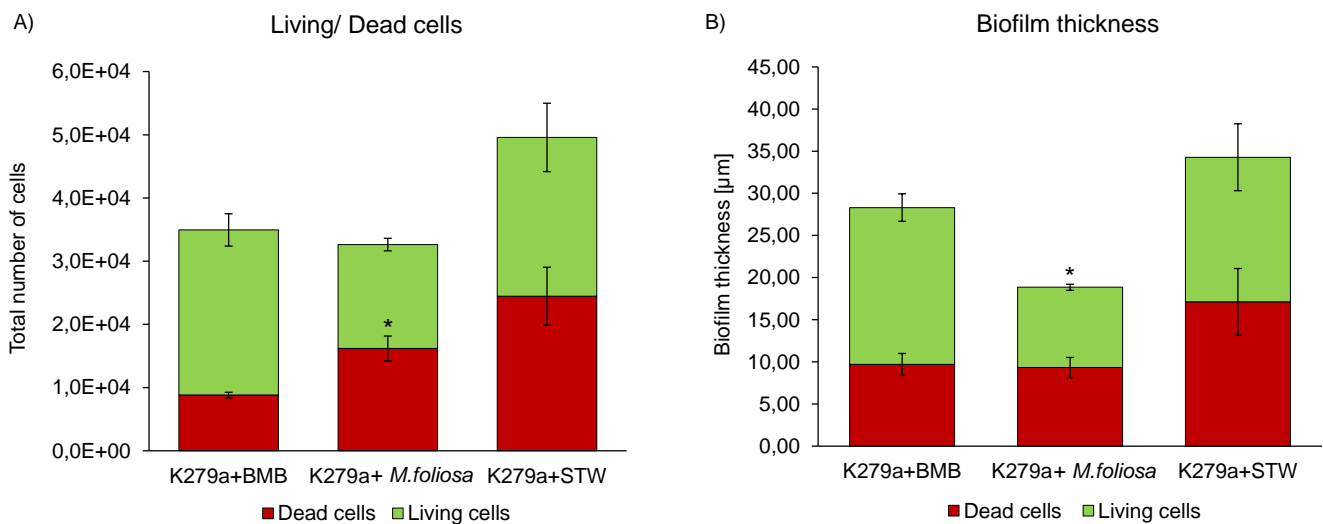


**Figure 5: Analysis of the confocal microscopic images of *Stenotrophomonas maltophilia* biofilms treated with sterile filtered supernatant of an enrichment culture with *M. foliosa*, STW, and BMB (control).** The total number of cells (A) and biofilm mean thickness (B) are represented in green (living cells) and red (dead cells). The number of dead cells was significantly higher with a p-value of 0.01 in the sample with *M. foliosa* than in the control and the biofilm thickness was significantly reduced with a p-value of 0.04. The data are mean values of at least three replicates. The error bars indicate simple standard deviations (original figure from Peters et al., 2023, modified by M. Peters).

The number of dead cells in this sample was significantly higher with a  $p$ -value of 0.01. The analysis of the biofilm thickness also proved the effectiveness of the supernatant on K279a. The biofilm of the *M. foliosa* sample was significantly reduced by about 33 % with a  $p$ -value of 0.04 (Figure 5 B). In contrast to the sample K279a+STW22, which showed merely the same number of dead and living cells, and no reduction of the biofilm thickness.

### 3.4 Metagenome-based microbial community analyses

Sequencing of the metagenome of the microbial community from *M. foliosa* and STW22 enabled an overview of what organisms are prevalent in these consortia and which biomolecules. Raw data of the *M. foliosa* community contained 83,679,656

sequences with a GC content of 42 % (Table 6). The assembled metagenome was analyzed with the Integrated Microbial Genomes & Microbiomes (IMG ID 222864) database and covered 42,166,744 bp with a GC count of 48.39 % and 47,903 protein-coding genes (Table 6). Sequencing of the shark tank community (IMG ID 222865) provided 87,355,173 sequences with a GC content of 45%. The investigation with IMG database showed 74,400,095 bp with a GC count of 52.13 % and 85,886 protein-coding genes, almost twice the number in the coral metagenome.

**Table 6: Overall numbers of sequences and contigs** generated for metagenome analysis of microbial communities from *Montipora foliosa* and from a shark tank (original table from Peters et al., 2023, modified by M. Peters).

Parameter	Value <i>M. foliosa</i>	Value STW
<b>Reads Illumina 1.9 (filtered)</b>		
Total sequences	83,679,656	87,355,173
Duplicates (%)	37.45	32.80
GC (%)	42	45
<b>IMG ID metagenome statistic</b>		
IMG ID	222864	222865
Number of bases	42,166,744	74,400,095
GC count (%)	48.39	52.13
Number of protein-coding genes	47,903	85,886
% of assembled protein-coding genes	98.87	99.05

The phylogenetic distribution pointed out which organisms are the key players in the consortia (Figures 6 and 7). The most abundant bacterial phylum in the *M. foliosa* community (Figure 6) was Firmicutes with 23.4 %, followed by Alphaproteobacteria (18.0 %), Gammaproteobacteria (2.8 %), and Actinobacteria (0.7 %). Firmicutes were split up into four genera: *Paenibacillus* (13.4 %), *Bacillus* (8.0 %), *Sutcliffeiella* (1.0 %), and *Cytobacillus* (0.2 %). The Alphaproteobacteria were represented by *Ruegeria* (16.1 %), *Labrenzia* (0.6 %), *Roseibium* (0.5 %), *Leisingera* (0.1 %), and 0.6 % unclassified Rhodobacteraceae. In addition, 2.8 % *Microbulbifer* (Gammaproteobacteria) and 0.7 % *Gordonia* (Actinobacteria) were found. In total, the number of different species within the metagenome was limited to 55.

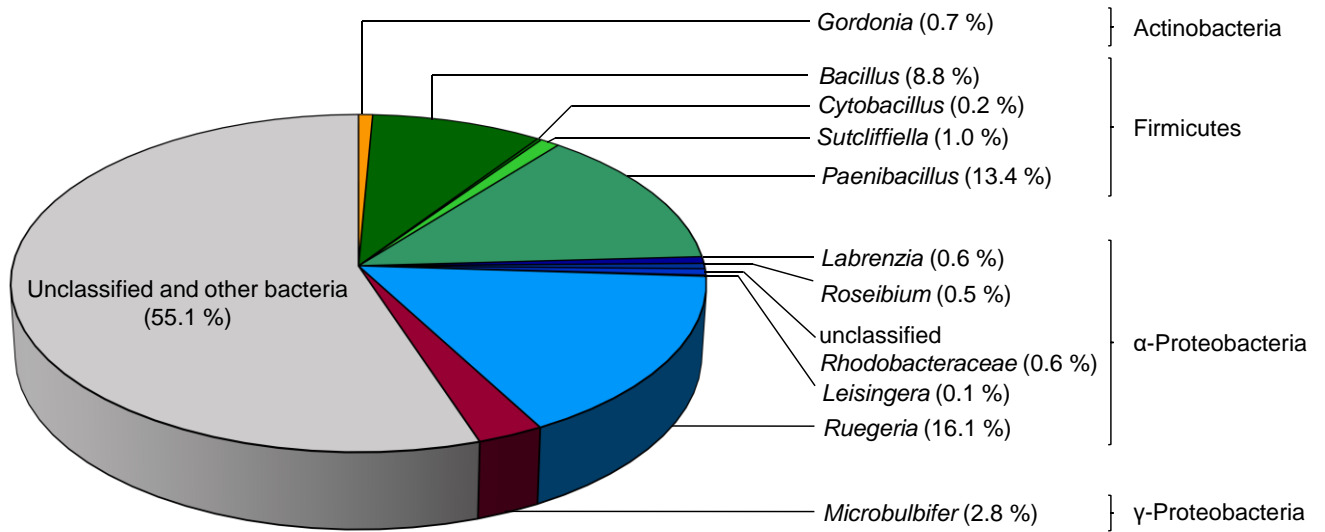


**Figure 6: Phylogenetic analysis of microbial communities from an enrichment culture with *M. foliosa*.** Representation of the percentage distribution of different genera within the metagenome. It was analyzed with the Integrated Microbial Genomes & Microbiomes (IMG, 222864) database (22.02.22) (original figure from Peters et al., 2023).

The microbial community of the STW22 culture was composed of 30.3 % Alphaproteobacteria, and 30.2 % Gammaproteobacteria (Figure 8). Mainly species of the genera *Maritalea* (7.0 %), *Ahrensia* (4.8 %), *Sulfitobacter* (4.2 %), *Tepidicaulis* (3.6 %), *Roseovarius* (3.4 %), and *Phaeobacter* (3.0 %) within the Alphaproteobacteria were found. The Gammaproteobacteria were represented basically by *Marinobacter* (6.8 %), *Vibrio* (6.4 %), *Cocleimonas* (5.6 %), *Pseudoalteromonas* (4.1 %), *Spongiibacter* (3.3 %), and *Idiomarina* (2.7 %). Overall, about 138 different species within the STW22 community were detected.

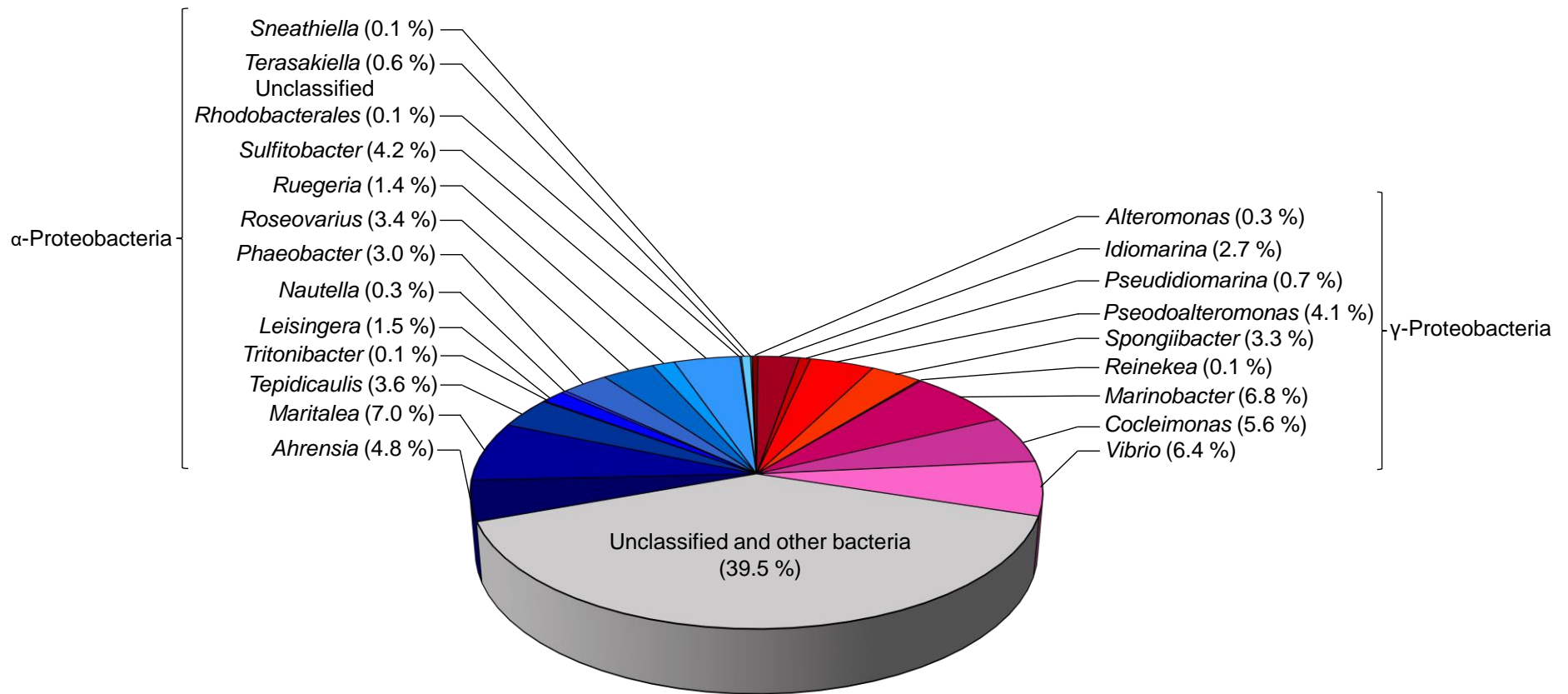


**Figure 7: Phylogenetic analysis of microbial communities from an enrichment culture with water from a shark tank.** Representation of the percentage distribution of different genera within the metagenome. It was analyzed with the Integrated Microbial Genomes & Microbiomes (IMG, 222865) database (21.09.22).

For further investigations, the COG (Clusters of Orthologous Groups) database was used, and functional analysis of both metagenomes was performed (Table 7).

**Table 7: Key features observed in the microbial communities from *Montipora foliosa* and a shark tank** using IMG data analysis (original table from Peters et al., 2023, modified by M. Peters). Data shown in % of all hits.

Trait	<i>M. foliosa</i>	STW
Amino acid metabolism	10.02	10.05
Biosynthesis of other secondary metabolites	1.09	1.04
Carbohydrate metabolism	8.94	8.22
Cell motility	1.57	2.15
Drug resistance	1.04	1.03
Energy metabolism	5.96	5.8
Folding, sorting and degradation	1.79	1.76
Global and overview maps	27.01	26.92
Glycan biosynthesis and metabolism	1.29	1.35
Lipid metabolism	3.08	2.95
Membrane transport	7.33	6.82
Metabolism of cofactors and vitamins	5.64	5.79
Metabolism of other amino acids	2.62	2.83
Metabolism of terpenoids and polyketides	1.59	1.75
Nucleotide metabolism	3.87	3.72
Replication and repair	2.04	2.03
Signal transduction	4.16	4.35
Translation	3.1	3.02
Xenobiotics biodegradation and metabolism	2.22	2.57
Others	5.64	5.85
Total	100	100

About 25 % of all key features in the coral community were represented by amino acid, carbohydrate, and energy metabolism. In addition, membrane transport and metabolism of cofactors and vitamins were highlighted with nearly 13 % (Table 7). Signal transduction was represented at 4%, nucleotide metabolism with nearly 4 %, and like lipid metabolism and translation mechanisms with 3 %. The metabolism of other amino acids, replication, repair, and xenobiotics biodegradation was observed at about 2 %. The following key features were all represented with 1 %: biosynthesis of

secondary metabolites, cell motility, drug resistance, folding, sorting, degradation, glycan biosynthesis, and metabolism of terpenoids and polyketides. Comparable results were provided with the functional analysis of the STW22 metagenome (Table 7). Amino acids, carbohydrates, cofactors, vitamins, and energy metabolism accounted for nearly one-third of the key features. Followed by membrane transport (7 %), signal transduction (4 %), nucleotide metabolism (4 %), and translation mechanisms (3 %). Metabolism of lipids, other amino acids, terpenoids and polyketides, cell motility, xenobiotics biodegradation and metabolism, replication, repair, folding, sorting, and degradation were represented by about 2 %. Furthermore, biosynthesis of other secondary metabolites, drug resistance, and glycan biosynthesis and metabolism, were detected in each case with about 1 % of all key features.

In the next step, the focus was on the overall enzymes potentially involved in anti-biofilm activity. The COG-based search showed a range of diverse biomolecules, described for anti-biofilm and Quorum quenching mechanisms in literature.

**Table 8: Key features of putative antimicrobial and Quorum quenching active enzymes observed in the bacterial communities from *Montipora foliosa* and a shark tank** using a COG-based analysis (original table from Peters et al., 2023, modified by M. Peters). Data shown in total number of hits per 100 Mb.

<b>Enzymes</b>	<b><i>M. foliosa</i></b>	<b>STW</b>
<b>Chelataes</b>	49	101
Magnesium chelataes	15	38
<b>Deacetylases</b>	175	279
<b>Deaminases</b>	224	394
Cytosine/adenosine deaminase-related metal-dependent hydrolases	33	59
<b>Decarboxylases</b>	195	337
Arginine decarboxylases	14	30
<b>Endonucleases</b>	181	363
Restriction endonucleases	22	79
<b>Lyases</b>	472	806
<b>Lysozymes</b>	10	34
<b>Polyketide synthases</b>	14	40
<b>Proteases</b>	515	958
Serine proteases	111	187
Metalloproteases	18	20
<b>Quorum quenching</b>		
<b>Acyases</b>	148	282
<b>Lactonases</b>	39	76
6-phosphogluconolactonases	20	25
<b>Dienelactone hydrolases</b>	16	39
<b>Oxidoreductases</b>	605	1149
Fe-S oxidoreductases	51	101
FAD-dependent oxidoreductases	32	101

In total, 49 chelataes, 175 deacetylases, 224 deaminases, 195 decarboxylases, 181 endonucleases, 472 lyases, 10 lysozymes, and 14 polyketide synthases for the bacterial community from *M. foliosa* were detected (Table 7). One group accounted for most of these enzymes, namely 515 proteases. Beyond that, we found a few Quorum Quenching enzymes, such as 148 acylases, 39 lactonases, 16 dienelactone hydrolases, and 605 oxidoreductases. Remarkable were the results of the investigation of the shark tank community (Table 8). Almost twice the number of each anti-biofilm enzyme class was detected. In detail, 101 chelataes, 279 deacetylases, 394

deaminases, 337 decarboxylases, 363 endonucleases, 806 lyases, 34 lysozymes, 40 polyketide synthases, and 958 proteases. The group of Quorum quenching enzymes was represented by 282 acylases, 76 lactonases, 39 diene lactone hydrolases, and 1,149 oxidoreductases.

### 3.5 Transcriptome analysis of *Stenotrophomonas maltophilia* biofilm after treatment with different supernatants

An investigation of the transcriptome of *S. maltophilia* K279a was performed to understand the mechanisms during biofilm formation and inhibition. One aim of this study was the identification of genes involved in this process and the detection of an effect of *M. foliosa* and STW22 supernatant on gene level as well. The Next-Generation Sequencing (NGS) of the biofilm treated with *M. foliosa* supernatant resulted in 8,895,226 sequences with an average length of 149 bp and a GC content of 62.50 %. The sample with STW22 provided 9,558,336 sequences with an average length of 147 bp and 54.67 % GC content (Table 9).

**Table 9: Overall numbers of sequences and contigs generated for the transcriptome datasets of *Stenotrophomonas maltophilia* K279a biofilm** (original table from Peters et al., 2023, modified by M. Peters).

	<b>K279a controle</b>	<b>K279a + <i>M. foliosa</i></b>	<b>K279a + STW22</b>
<b>Reads Illumina (filtered)</b>			
Total no.	8,072,838	8,895,226	9,558,336
Average length (bp)	147	149	147
Duplicates (%)	72.89	79.28	74.04
Fails (%)	25.76	28.79	28.79
GC (%)	57.33	62.50	54.67

The circular genome mapping of *Stenotrophomonas maltophilia* K279a was generated using the Circular Genome Viewer tool within PATRIC, the Pathosystems Resource Integration Center ([www.patricbrc.org](http://www.patricbrc.org)) (Figures 8 and 9). Both circular genome maps show all up- and down-regulated genes of K279a biofilm after treatment with the supernatant of either *M. foliosa* or STW enrichment culture, mapped on *S. maltophilia* transcriptome.



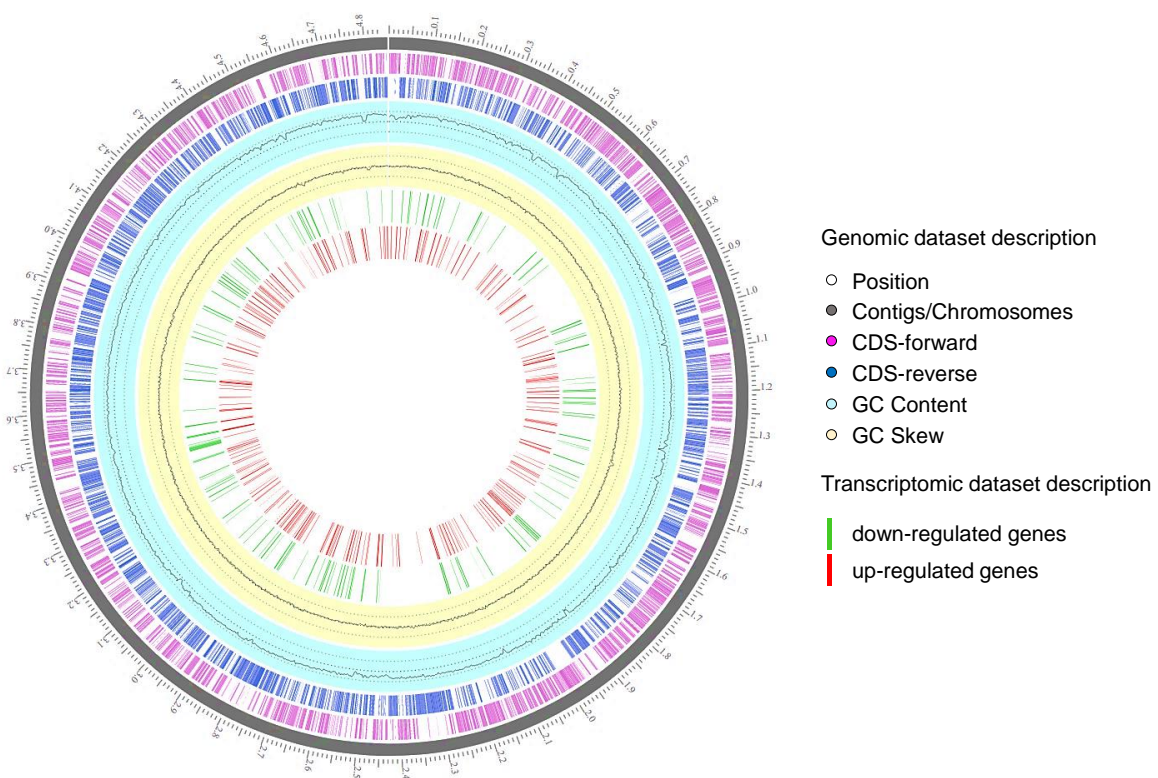


**Figure 8: Transcriptome analysis/ Circular genome mapping of *Stenotrophomonas maltophilia* K279a after treatment with supernatant of *M. foliosa* enrichment culture (GenBank: AM743169.1).** Moving inward, the subsequent two rings show CDSs in forward (magenta) and reverse (blue) strands. Cyan and yellow plots indicate GC content and a GC skew  $[(GC)/(G+C)]$ . Transcriptomic dataset description - red: up-regulated genes; green: down-regulated genes (original figure from Peters et al., 2023).

It was noticeable that in the case of the *M. foliosa* sample, significantly more genes (up- and down-regulated) could be mapped to the transcriptome (Figure 8). The generated data for the STW sample was not sufficient to make a statement about the effect on *S. maltophilia* biofilm. Based on these results, the following transcriptome investigation was only performed for the *M. foliosa* sample and the STW sample was excluded.

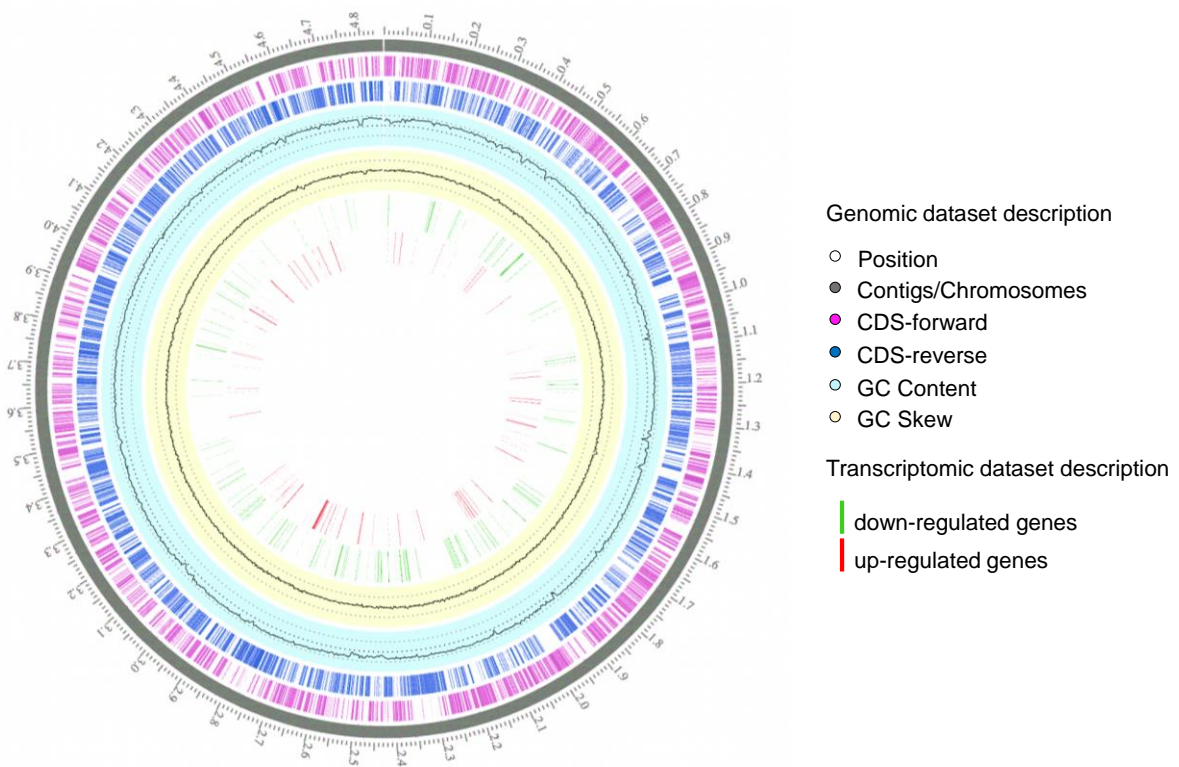


**Figure 9: Transcriptome analysis/ Circular genome mapping of *Stenotrophomonas maltophilia* K279a after treatment with supernatant of STW enrichment culture (GenBank: AM743169.1).** Moving inward, the subsequent two rings show CDSs in forward (magenta) and reverse (blue) strands. Cyan and yellow plots indicate GC content and a GC skew [(GC)/(G+C)]. Transcriptomic dataset description - red: up-regulated genes; green: down-regulated genes.

A deep analysis of the transcriptome dataset confirmed that K279a reacted to the supernatant of the *M. foliosa* enrichment culture. There was evidence of biofilm formation, but also of stress response in general (Figure 10, Table 10). The distribution of gene expression between *S. maltophilia* K279a incubated with the supernatant of *M. foliosa* enrichment culture and control sample is represented by the volcano plot (Figure 10A). The volcano plot was constructed to compare the two groups using ggVolcanoR. A total of 1,530 differentially expressed genes (DEGs) were identified from the dataset (Figure 10A). Among them, 612 and 918 genes were up-regulated and down-regulated, respectively, between the two groups according to their  $\log_2FC$  and  $p$ -values.

**Table 10: Heatmap of expression levels of differentially expressed genes response of *Stenotrophomonas maltophilia* K279a to *Montipora foliosa* enrichment culture.** RNA-Seq Analysis was performed using the tuxedo strategy, the heatmap was generated using the Expression Import Service of the Pathosystems Resource Integration Center, PATRIC, the absolute value of log<sub>2</sub> Ratio >1.5 (original table from Peters et al., 2023).

	Refseq Tag/Gene	Locus	Product	Category
	SmLt1429, nfi		Endonuclease V *	Antimicrobial and defense mechanisms
	SmLt1648		Monooxygenase, FAD-binding *	
	SmLt0603		Peptidase M14	
	SmLt2603		Predicted mannuronate transporter	Carbohydrate transport and metabolism
	SmLt1335		RelE-like translational repressor toxin *	
	SmLt1196		Xylose isomerase-like TIM-barrel protein	
	SmLt2601		Alginate lyase	Coenzyme transport and metabolism
	SmLt0260		Nicotinamide phosphoribosyltransferase	
	SmLt2421, arsC		Arsenate reductase, glutaredoxin-coupled *	
	SmLt0177, arsC		Arsenate reductase, thioredoxin-coupled*	Inorganic ion transport and metabolism
	SmLt2424, arsC2		Arsenate reductase, thioredoxin-coupled*	
	SmLt2422, arsH		Arsenic resistance protein, ArsH *	
	SmLt2425, arsB		Arsenical-resistance protein, ACR3 *	
	SmLt1428		Cobalt/zinc/cadmium resistance protein, CzcD *	
	SmLt2713		Iron acquisition protein *	
	SmLt3740		Ferric enterobactin receptor *	
	SmLt0602		TonB-dependent receptor *	Lipid transport and metabolism
	SmLt4240, accB		Biotin carboxyl carrier protein of acetyl-CoA carboxylase	
	SmLt2367		Outer membrane lipoprotein	
	SmLt1030, acpP		Acyl carrier protein	Methionine biosynthesis
	SmLt0767, metF		5,10-methylenetetrahydrofolate reductase*	
	SmLt3176, metH2		5-methyltetrahydrofolate-homocysteine methyltransferase*	
	SmLt2511		4-carboxymuconolactone decarboxylase, AhpD *	Oxidative stress related mechanisms
	SmLt0841, ahpC		Alkyl hydroperoxide reductase protein C *	
	SmLt0840, ahpF		Alkyl hydroperoxide reductase protein F *	
	SmLt2882, cpo		non-heme chloroperoxidase *	
	SmLt0593		Peptide-methionine (R)-S-oxide reductase, MsrB *	
	SmLt0186		Glyoxalase, methylglyoxal metabolism *	
	SmLt0605, rhlE1		ATP-dependent RNA helicase, RhlE	
	SmLt0004, uvrF		DNA recombination and repair protein, RecF	Replication, recombination and repair
	SmLt1336		Prophage integrase	
	SmLt1323		Mobile element protein	
	SmLt3900, rpoE		RNA polymerase ECF-type sigma factor	Signal transduction and regulation mechanisms
	SmLt1334		Antitoxin to RelE-like translational repressor toxin *	
	SmLt1158		Iron-sulfur cluster regulator, IscR *	
	SmLt4370, glnB		Nitrogen regulatory protein P-II, GlnK	
	SmLt2053		Transcriptional regulator for fatty acid degradation, TetR family	
	SmLt3021		Transcriptional regulator, AcrR family	
	SmLt2148		Transcriptional regulator, ArsR family	
	SmLt3089		Transcriptional regulator, LysR family	
	SmLt4660		Transcriptional regulator, MarR family	
	SmLt3012		Transcriptional regulator, MerR family	
	SmLt1898		Transcriptional regulator, Xre family	
	SmLt2256, cheW		Positive regulator of CheA protein, CheW *	Transporter, efflux pumps and secretion systems
	SmLt0790		Arabinose efflux permease	
	SmLt3942, dctA		Na <sup>+</sup> /H <sup>+</sup> -dicarboxylate symporter *	
	SmLt2851,		Spermidine export protein, MdtI, multidrug resistance	
	SmLt2852,		Spermidine export protein, MdtJ, multidrug resistance	
	SmLt0549,		MFS-type transporter	
	SmLt2420,		MFS-type transporter	
	SmLt0548,		MFS-type transporter	
	SmLt2119,		MFS-type transporter	
	SmLt1350		autotransporter related to pathogenesis	
	SmLt1001, arsC		autotransporter related to pathogenesis	
	SmLt2874		Flp pilus assembly protein, TadB *	
	SmLt2869		Flp pilus assembly protein, TadG *	

A)

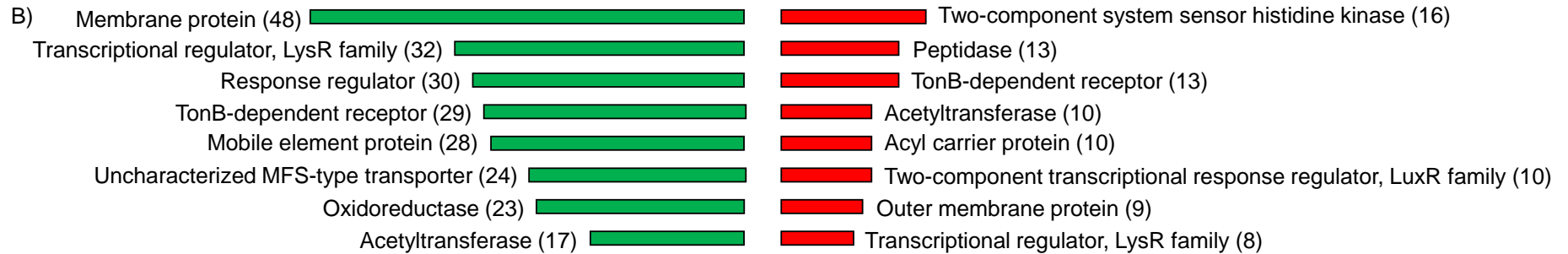
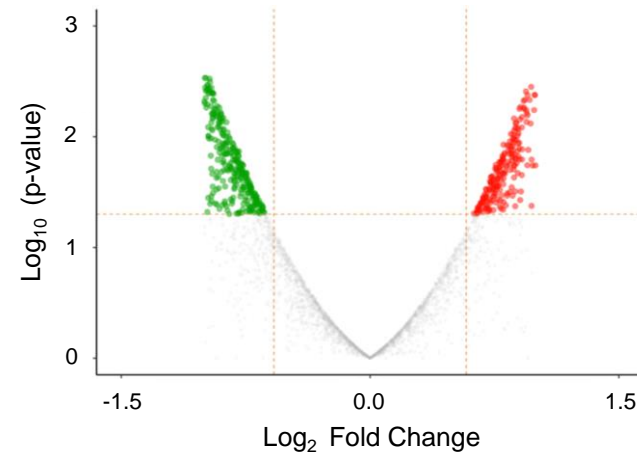


**Figure 10: Differentially expressed genes (DEGs) in *Stenotrophomonas maltophilia* K279a in response to *M. foliosa* enrichment culture compared with the control dataset, all genes were selected with  $|\log_2(\text{fold change})| \geq 1.5$ .** (A) Volcano plot highlights the DEGs in *S. maltophilia* K279a, x-axis:  $\log_2$ , large-scale fold changes; y-axis:  $-\log_{10}$  of the  $p$ -value showing the statistical significance. Each point corresponds to one gene. The points above the vertical and horizontal dotted lines represent  $\log_2\text{FC} \geq 0.58$  and  $p\text{-value} < 0.05$ . The volcano plot was generated using a Shiny app ggVolcanoR. (B) Functional description of highly active up- (red) and down- (green) regulated genes of *S. maltophilia* K279a in response to *M. foliosa* enrichment culture (original figure from Peters et al., 2023).

The strongest and most significantly differentially regulated genes were 32 counts of down-regulated and 8 counts of up-regulated genes for transcriptional regulators in the LysR family (Figure 10B). Besides that, there were 13 gene counts for peptidases, 10 for acyl carrier proteins, and 10 for two-component transcriptional response regulators which were up-regulated. Interestingly, several counts for TonB-dependent receptors (13 up-regulated and 29 down-regulated) could be detected. The largest group of up-regulated genes was represented by two-component system sensor histidine kinases (16). The down-regulated genes were dominated by 48 counts of membrane proteins. In contrast, there were only a few outer membrane proteins (9) which were up-regulated. In addition, the analysis of down-regulated genes resulted in response regulators (30), mobile element proteins (28), uncharacterized MFS-type transporter (24), and oxidoreductases (23). The group of acetyltransferases was represented by 17 counts of down-regulated and 10 counts of up-regulated genes. More details about all up- and down-regulated genes related to the response of K279a to the *M. foliosa* culture have been listed in Table 10. It could be identified genes linked to defense mechanisms, carbohydrate, coenzyme, ion and lipid transport and metabolism, methionine biosynthesis, oxidative stress-related mechanisms, repair mechanisms, signal transduction, transporter, efflux pumps and secretion systems. In detail, two genes coding for the metal resistance proteins Acr3 and CzcD, and one gene coding for an antitoxin to RelE-like translational repressor toxin were highly up-regulated. In addition, two genes for major facilitator superfamily (MFS) transporter systems and one gene for an autotransporter related to pathogenesis, were up-regulated as well. The deeper analysis of antimicrobial and defense mechanisms revealed down-regulated antimicrobial enzymes like FAD-binding monooxygenase, endonucleases, and exonucleases. In addition, genes within inorganic ion transport and metabolism mostly covered iron acquisition, arsenic, and heavy metal resistance, which are known to be connected with biofilm formation (Farasin et al. 2017, Hoeft et al. 2010, Kang and Kirienko 2018, Teitzel and Parsek 2003). A series of genes connected to signal transduction and regulation mechanisms were down-regulated. These genes included transcriptional regulators, chemotaxis genes, and iron-sulfur cluster proteins that act as a sensor of the environment and enable the organism to adapt to the prevailing conditions (Crack et al. 2012, Tout et al. 2015).

The generated data about the *M. foliosa* sample were convincing and indicated that the supernatant had a strong effect on *S. maltophilia* biofilm. Consequently, a deeper analysis of the secreted proteins in the supernatant followed.

### **3.6 Secretome-based analysis of *M. foliosa* enrichment culture**

*M. foliosa* and STW22 supernatants were both investigated via mass spectrometry. The STW22 sample gave inconclusive results and was excluded from all further testing.

The total supernatant proteome of the *M. foliosa* sample resulted in 338 peptides with masses between 31 and 159 kDa (Table 11). The data comprised different hydrolases, including proteases, alpha-amylases, glutathione hydrolase proenzymes, chitosanases, oligopeptide-binding proteins, pectate lyases, glucuronoxylanases, and phosphoesterases. The most abundant enzymes were proteases e.g., 77 metalloproteases, 46 serine proteases, 32 neutral proteases, 17 cell wall-associated proteases, and 13 extracellular proteases. Nearly all hydrolases detected in the proteome originated from *Bacillus* strains.

**Table 11: Detected peptides in the supernatant of the enrichment culture with *M. foliosa* using electrospray ionization mass spectrometry coupled with liquid chromatography** (filtered data, original table from Peters et al., 2023).

Accession (NCBI)	Number of peptides	Avg. mass (DA)	Description
P68734 NPRES_BACPU	32	32674	Neutral protease NprE OS= <i>Bacillus pumilus</i>
P68736 NPRES_BACSU	32	56522	Bacillolysin OS= <i>Bacillus subtilis</i> (strain 168)
P68735 NPRES_BACSA	32	56522	Bacillolysin OS= <i>Bacillus subtilis</i> subsp. <i>amylosacchariticus</i>
P00691 AMY_BACSU	25	72378	Alpha-amylase OS= <i>Bacillus subtilis</i> (strain 168)
P54422 GGT_BACSU	24	64189	Glutathione hydrolase proenzyme OS= <i>Bacillus subtilis</i> (strain 168)
P04189 SUBT_BACSU	16	39479	Subtilisin E OS= <i>Bacillus subtilis</i> (strain 168)
P00783 SUBT_BACSA	15	39467	Subtilisin amylosacchariticus OS= <i>Bacillus subtilis</i> subsp. <i>amylosacchariticus</i>
P29142 SUBT_GEOSE	15	39495	Subtilisin J OS= <i>Geobacillus stearothermophilus</i>
P39790 MPR_BACSU	13	33842	Extracellular metalloprotease OS= <i>Bacillus subtilis</i> (strain 168)
P63186 GGT_BACNA	19	64070	Glutathione hydrolase proenzyme OS= <i>Bacillus subtilis</i> subsp. <i>natto</i>
O07921 CHIS_BACSU	14	31497	Chitosanase OS= <i>Bacillus subtilis</i> (strain 168)
P24141 OPPA_BACSU	12	61525	Oligopeptide-binding protein OppA OS= <i>Bacillus subtilis</i> (strain 168)
P39116 PLY_BACSU	12	45498	Pectate lyase OS= <i>Bacillus subtilis</i> (strain 168)
Q45070 XYNC_BACSU	12	47337	Glucuronoxylanase XynC OS= <i>Bacillus subtilis</i> (strain 168)
P25152 BSAP_BACSU	17	49450	Aminopeptidase YwaD OS= <i>Bacillus subtilis</i> (strain 168)
P54423 WPRA_BACSU	17	96488	Cell wall-associated protease OS= <i>Bacillus subtilis</i> (strain 168)
P29141 SUBV_BACSU	13	85608	Minor extracellular protease vpr OS= <i>Bacillus subtilis</i> (strain 168)
O34313 NTPES_BACSU	18	159705	Trifunctional nucleotide phosphoesterase protein YfkN OS= <i>Bacillus subtilis</i> (strain 168)

The fractionation with the FPLC system refined the search for the responsible enzymes in the supernatant of the *M. foliosa* enrichment culture. We could identify several fractions that contained putative proteins (Figure 12A). For determination of the protein amount and for separation an SDS-Page was prepared and stained with Pierce™ Silver Stain Kit (Thermo Fisher Scientific, Waltham, MA, USA, Figure 11).

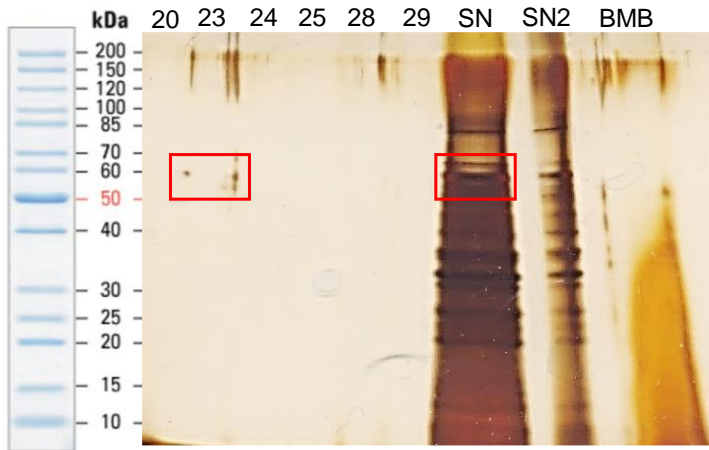


**Figure 11: SDS-Page with fractions of the *M. foliosa* culture after fractionation with the FPLC system.** The SDS-Page was stained with Pierce™ Silver Stain Kit (Thermo Fisher Scientific, Waltham, MA, USA). The PageRuler™ Unstained Protein Ladder (Thermo Fisher Scientific, Waltham, MA, USA) was used as a marker. 20 – 29: Fractions after FPLC clean-up. SN/ SN2: Supernatant of the *M. foliosa* enrichment culture. BMB: Bacto Marine Broth as negative control. The red boxes mark the interesting proteins on the level of 60 kDa.

Fraction 23 showed a slight band on the level of 60 kDa just like the control with the whole supernatant of the *M. foliosa* culture.

To verify the activity of this fraction, biofilm prevention assays with *Stenotrophomonas maltophilia* K279a were performed. In Figure 12B the tested 8 fractions and the undiluted supernatant are shown. All samples were compared to the strain with potassium phosphate buffer (pH 7.0), which acted as a negative control.



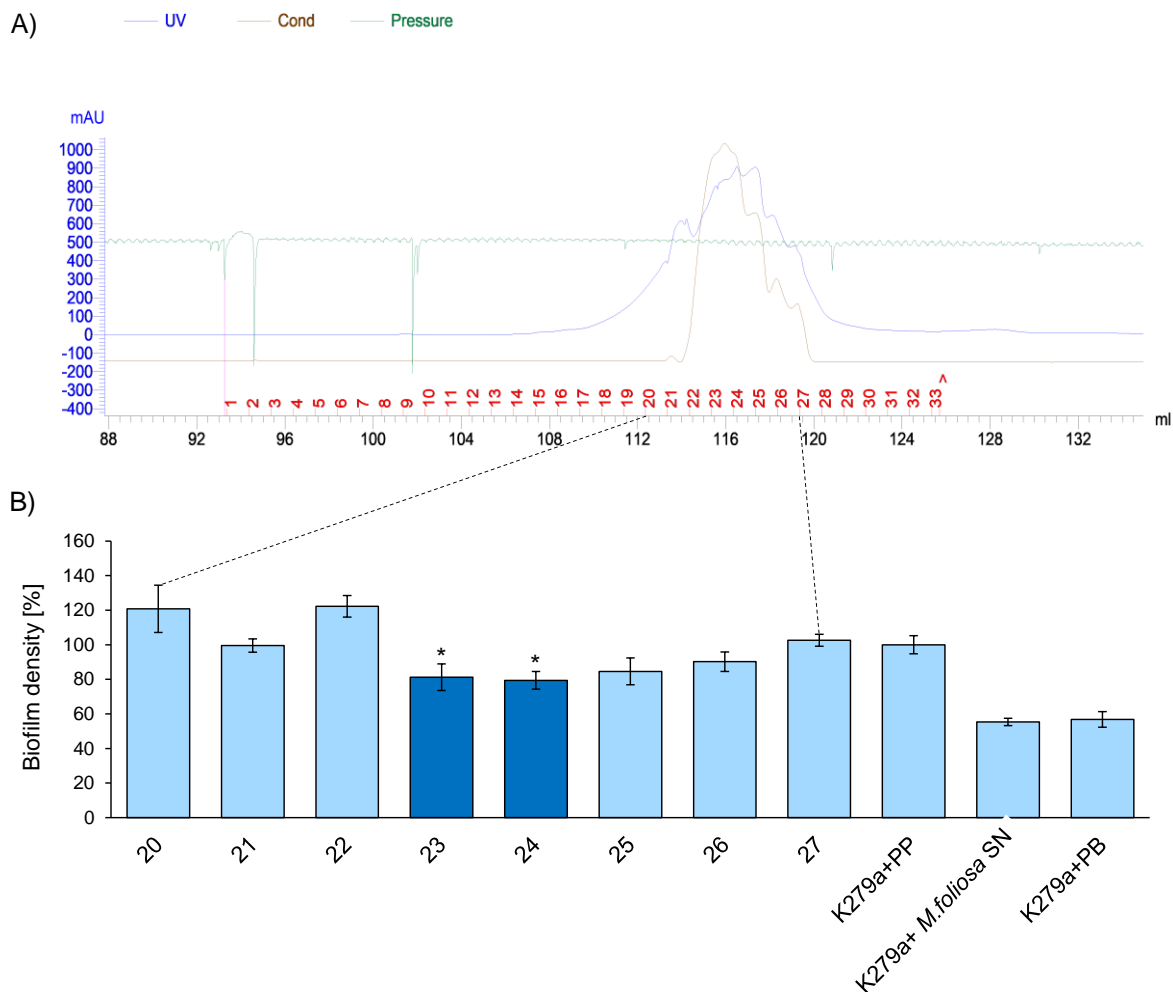


**Figure 12: (A) Chromatogram of the *Montipora foliosa* culture after fractionation with the FPLC system and a Superdex® 200 10/300 GL gel filtration column.** The supernatant was fractionated into 33 fractions. Potassium phosphate buffer pH 7.0 was the moving fluid. (B) Biofilm prevention assay with *Stenotrophomonas maltophilia* K279a treated with FPLC fractions of the *M. foliosa* enrichment culture. The K279a culture was incubated with fractions for 24 h in 96-well plates. The biofilm was stained with 0.5 % crystal violet and the density was measured at a wavelength of 595 nm. 20 – 27: Fractions after FPLC clean-up. K279a+PP: *S. maltophilia* with potassium phosphate buffer. K279a+*M. foliosa* SN: *S. maltophilia* incubated with the whole supernatant of the *Montipora foliosa* culture. K279a+PB: Positive control, *S. maltophilia* treated with a protease from *Bacillus licheniformis*. The fractions 23 and 24 significantly reduced the biofilm density with a p-value of  $2.2 \times 10^{-4}$  and  $5.6 \times 10^{-5}$ , respectively. The data are mean values of at least three replicates. The error bars indicate simple standard deviations (original figure from Peters et al., 2023).

The whole supernatant could reduce the biofilm density by up to 40 %, just as the commercially acquired protease (subtilisin A) from *Bacillus licheniformis* (P5380, Sigma-Aldrich, Merck KGaA, Darmstadt, Germany). The fractions 23 and 24 still significantly decreased the biofilm by about 20 % with a p-value of  $2.2 \times 10^{-4}$  and  $5.6 \times 10^{-5}$ , respectively, in contrast to the negative control (Figure 12B).

**Table 12: Most abundant proteins in the active fractions 23 and 24 of the enrichment culture supernatant with *Montipora foliosa*.** Based on a proteome analysis using electrospray ionization mass spectrometry coupled with liquid chromatography (filtered data, original table from Peters et al., 2023).

Accession (UniProt)	Number of sequences	Mass (DA)	Sequence coverage	Description
A0A1J9WHY4	68	100256	0.74	Microbial collagenase OS= <i>Bacillus cereus</i>
A0A0G3B7J6	10	110008	0.13	Microbial collagenase OS= <i>Bacillus cereus</i>
A0A2B2M9I7	4	109685	0.07	Microbial collagenase OS= <i>Bacillus cereus</i>
A0A1J9WEP7	13	63716	0.28	Peptide ABC transporter substrate-binding protein OS= <i>Bacillus cereus</i>
A0A1Y6A081	3	63395	0.06	Peptide ABC transporter substrate-binding protein OS= <i>Bacillus cereus</i>
A0A0J7GMX8	3	120049	0.04	Collagen-binding protein OS= <i>Bacillus cereus</i>

The proteome analysis of these highly active fractions led to significant sequences of a putative microbial protease with a mass of 100 kDa and a sequence coverage of 0.74 (Table 12). A search with the data resource UniProt (universal protein database, <https://www.uniprot.org>, The UniProt Consortium 2021) resulted in the protease ColA, which originated from *Bacillus cereus* (Abfalter et al., 2016).

### 3.7 Phylogenetic assignment and structural analysis

The proteome investigation of the two fractions (fractions 23 and 24), as described in the previous section, revealed a potential metalloprotease with 38  $\alpha$ -helices and 17  $\beta$ -sheets and a catalytic  $Zn^{2+}$  in the active site (Figure 13A, Abfalter et al. 2016). Comparison of the metalloprotease with the collagenase ColA from *B. cereus* showed a high conformity on structure level (Figure 13B).

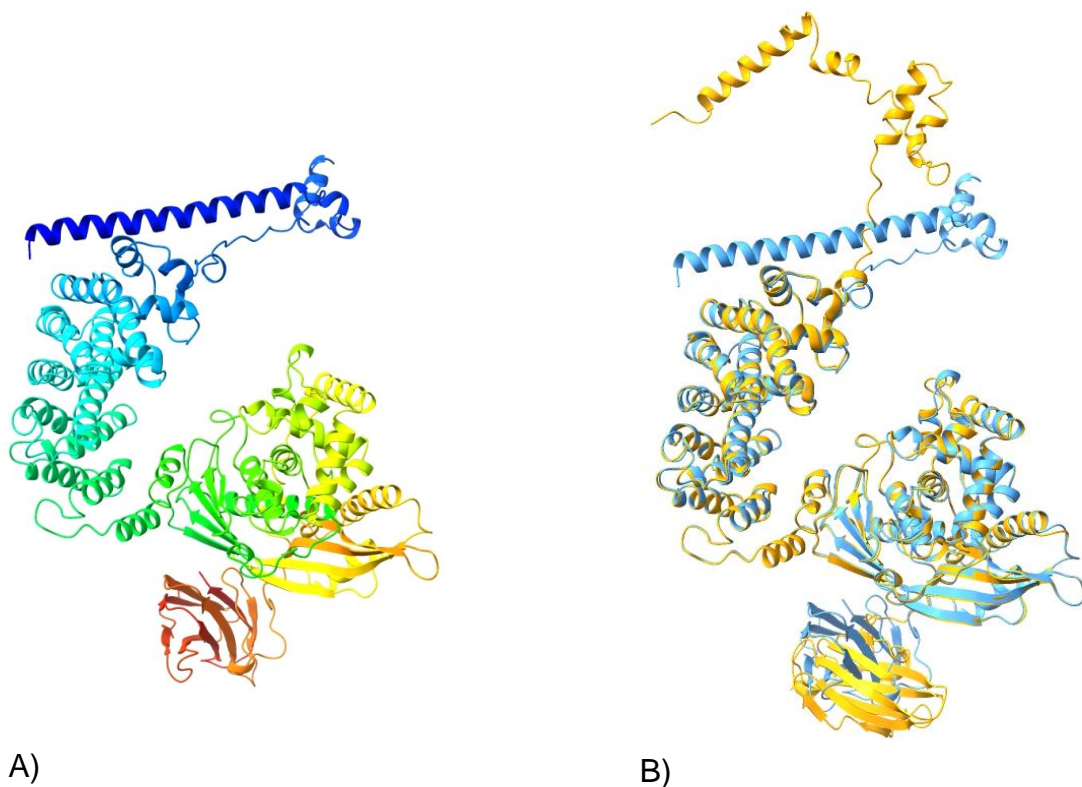


**Figure 13: (A) Structure prediction of microbial metalloprotease found in the proteome of the enrichment culture supernatant with *M. foliosa* with the help of Robetta (<https://robetta.bakerlab.org/>, Park et al., 2018). (B) Comparison of the predicted collagenase (light blue) with reference collagenase ColA from *Bacillus cereus* (ATCC 14579) (yellow, Abfalter et al., 2016), using UCSF ChimeraX (Pettersen et al., 2021).**

The phylogenetic analysis indicated that this protein belongs to the MEROPS family M9 of bacterial extracellular metalloproteases (BEMPs) (Figure 14, Wu and Chen 2011). In total 11 different groups or subgroups form this class of metalloproteases. Figure 15 shows a phylogenetic tree with a few examples for each group and assigns the enzyme detected in this study.

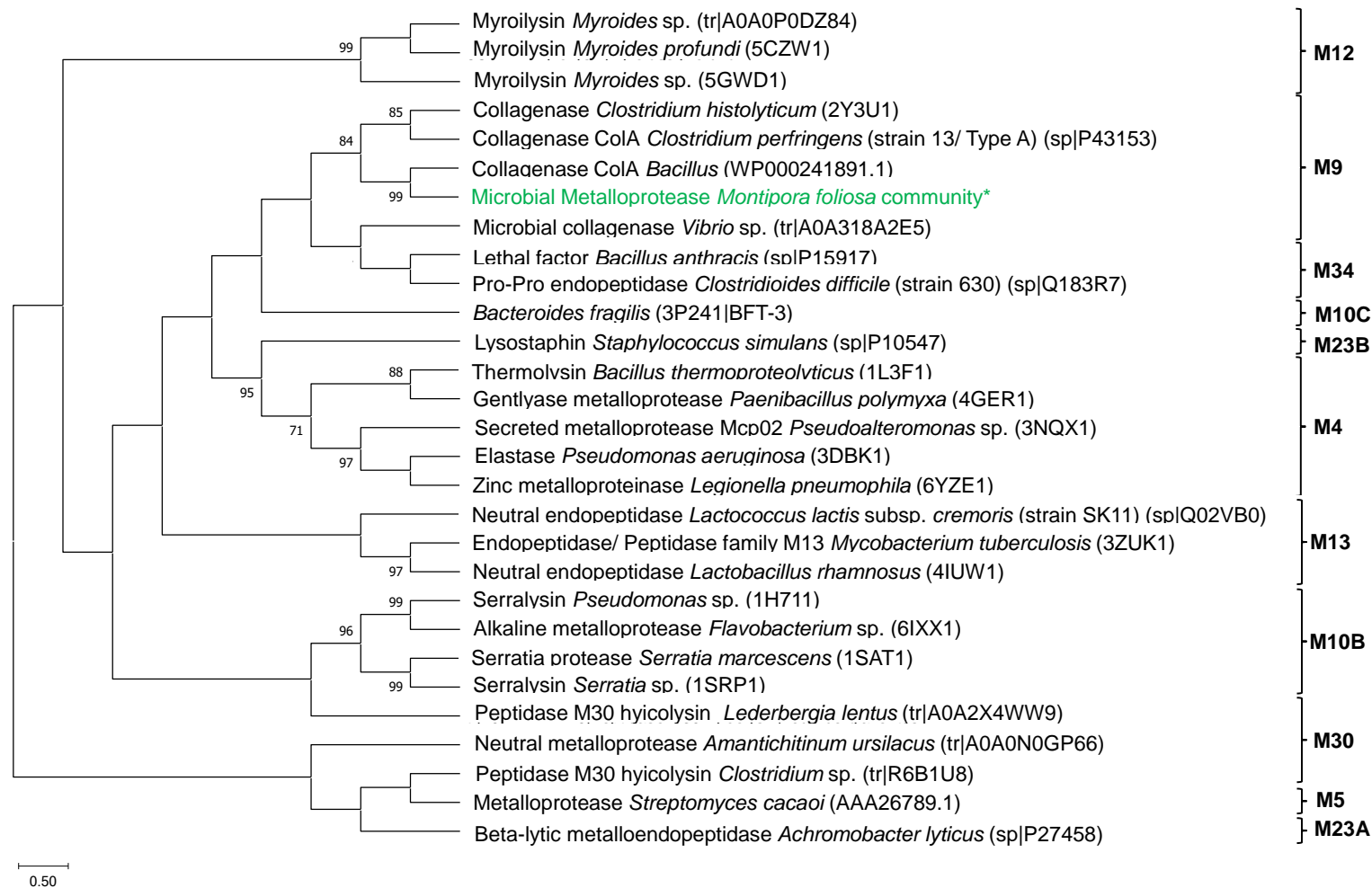


**Figure 14: Phylogenetic tree of bacterial extracellular metalloproteases (BEMPS) grouped in MEROPS families.** The phylogenetic tree was constructed with MegaX (Kumar et al., 2018) using the Maximum Likelihood method and JTT matrix-based model (Jones et al., 1992). The bootstrap consensus tree deviates from 1000 replicates (Felsenstein et al., 1985) after multiple alignments with T-Coffee (<https://tcoffee.org.eu/>, Notredame et al., 2000). The percentage of bootstrap resamplings  $\geq 70$  is illustrated on the branches. The scale bar represents the expected number of changes per amino acid position. This classification of metalloproteases is based on Wu and Chen, 2011. \*The predicted microbial metalloprotease from the bacterial community of *Montipora foliosa* is integrated into the MEROPS family M9 (original figure from Peters et al., 2023).

The M9 family contains, besides ColA, metalloproteases from *Vibrio* sp. or *Clostridium histolyticum*. This class of enzymes possesses a Zn<sup>2+</sup> in the active center and one activator domain, one peptidase domain, one or two polycystic kidney disease-like domains (PKD), and one to three collagen binding domains (CBD) and can degrade the major components in the extracellular matrix or on the cell surface in vertebrates, which make these proteins potentially useful in pharmaceutical applications (Matsushita and Okabe 2001, Eckhard et al. 2013, Abfalter et al. 2016).

## 4 Discussion

It is common knowledge that biofilms are causing serious problems in the medical field, especially in hospitals. Microorganisms, like *Pseudomonas aeruginosa* and *Stenotrophomonas maltophilia* are coming more into focus, because of their ability to colonize medical devices and immunocompromised patients (Sharma et al., 2013, Isom et al., 2022). *P. aeruginosa* and *S. maltophilia* strains evolved high resistance to a variety of antibiotics, e.g., quinolones and cephalosporins (Looney et al., 2009, Sanchez et al., 2015, Pang et al., 2018). Consequently, new approaches are required to find biomolecules and enzymes that disrupt the biofilm of such pathogens and prevent their spreading.

### 4.1 Discovering anti-biofilm enzymes from marine enrichment cultures

The marine environment offers a huge diversity of metabolites with unique characteristics like thermostability, pH, and salt tolerance (Zhang et al., 2021). This group of enzymes produced by marine organisms is of great interest to the biotechnology and the medical field (Vilela et al., 2021, Singh et al., 2016). Especially products that show activity against viruses, fungi, and bacteria (Vilela et al., 2021, Zhang et al., 2021). Therefore, marine samples were used for enrichment cultures in this study to access antimicrobials.

Preliminary biofilm assays of 5 samples narrowed down to two enrichment cultures supplemented with parts of the stony coral *M. foliosa* and water of a shark tank (STW22). Both showed strong prevention and degradation activity against *S. maltophilia*. In a comparison assay, the cultures confirmed the avoidance of biofilm formation by *S. maltophilia* but not of *P. aeruginosa*. In contrast, the deconstruction of a mature *P. aeruginosa* biofilm was observed by only STW cultures. In the next step, the antimicrobial effect especially on *S. maltophilia* by the *M. foliosa* and STW cultures was analyzed in detail via confocal microscopy. This investigation showed that the *M. foliosa* sample could partly dissolve the structure of the biofilm and significantly reduce living cells. Corals like *M. foliosa* live in symbiosis with microorganisms which are important for the health and resilience of these marine invertebrates (Peixoto et al., 2017, Shnit-Orland et al., 2009). Primarily studies about bacteria living in the mucus

showed the production of substances to compete with other microorganisms (Shnit-Orland et al., 2009, Pereira et al., 2017, Peixoto et al., 2017). The structure analysis of *S. maltophilia* biofilm after treatment with STW sample showed no comparable result. Especially the evaluation of the biofilm thickness and the number of living and dead cells could not confirm the results from the biofilm assays.

The overall investigations of the metagenomic dataset of our *M. foliosa* enrichment culture showed that Firmicutes was the dominant phylum. Several candidates belonging to the genus *Bacillus* showed antimicrobial activity by secretion of various metabolic components. For example, a *Bacillus firmus* culture extract could reduce the biofilm of methicillin-resistant *Staphylococcus aureus* (MRSA) by about 83 % (Modolon et al., 2020, Ghosh et al., 2022). Similarly, a group of enzymes produced by a marine *Bacillus licheniformis* is able to inhibit the biofilm formation of several microorganisms, like *Listeria monocytogenes*, *Escherichia coli*, and *S. aureus* (Díaz et al., 2022, Giri et al, 2019).

The bioinformatical analysis of the genomic datasets of *M. foliosa* and STW provided extensive insight into the microbial communities of these marine cultures. In total, the investigation of the STW sample resulted in a greater number of protein-coding genes. Since this was a water sample of a tank with various marine organisms, a larger dataset was expected. Nevertheless, both datasets showed numerous potential antimicrobial agents, especially proteases, endonucleases, chelatasases, and Quorum quenching active enzymes.

#### **4.2 Deep transcriptome analysis of *S. maltophilia* biofilm after stress induction**

With the tool of transcriptome analysis, the pathogen and its reaction to the added supplements could be analysed in detail. These datasets proved that the supernatant of the *M. foliosa* enrichment culture strongly influenced *S. maltophilia* K279a biofilm formation and induced stress response. A set of up-regulated genes was of particular interest, like the transcriptional regulator LysR, which acts as a virulence factor in pathogenic microorganisms and is crucial for biofilm formation and protease production (Wang et al., 2021, Islam et al., 2021). Besides, there were gene counts for TonB-dependent receptors, which are responsible for the uptake of iron-binding siderophores

(Fujita et al., 2019, Pawelek et al., 2006, Noinaj et al., 2010). Iron acquisition is indispensable for the transition of a pathogen from planktonic growth to biofilm building (Kang and Kirienko 2018, Zhang et al., 2021, Berlutti et al., 2005). A study of the transcriptomes of seven different *S. maltophilia* isolates also validated the up-regulation of genes coding for TonB-dependent receptors (Alio et al., 2020). Furthermore, several gene counts for sensor histidine kinases and peptidases were identified. These two enzyme groups are involved in the adaptation to changing conditions and stress response mechanisms, respectively (Khorchid and Ikura 2006, Culp et al., 2017). The up-regulation of a gene coding for the membrane protein Acr3 was detected. This permease acts as a metalloid antiporter and is responsible for arsenite resistance (Wawrzycka et al., 2017, Aaltonen and Silow 2008). Appropriately, the major facilitator superfamily (MFS) transporter system could be identified, known for the efflux of arsenicals as well (Garbinski et al., 2019). The CzcD protein, which was also highly up-regulated, acts in a similar functional way. It exports heavy metals, like cobalt, zinc, and cadmium, from the cytoplasm into the periplasm (Anton et al. 1999, Sullivan et al. 2021). Additionally, there was proof of a toxin-antitoxin system for preventing toxicity and probably building persister cells (Wang and Wood 2011, Kasari et al. 2013).

### **4.3 Biofilm degrading enzymes**

In general, a biofilm protects the bacterial cells against outside influences like chemicals and predators. Additionally, the physical barrier increases the antibiotic-resistant up to 1000-fold (Fleming and Rumbaugh 2017, Rogers et al., 2010). For this reason, the avoidance or destruction of biofilms has moved into focus in recent years, and new strategies have been tested. For example, polymeric surfaces with antibiotic or disinfect coatings should prevent the attachment of microbial cells. Over time, these surfaces become cracked and susceptible to biofilm formation again (Roy et al., 2018, Cattò and Cappitelli 2019).

Another strategy is to get access to the bacterial strains inside the biofilm and attack the structures of the extracellular matrix. Figure 14A illustrates a biofilm of microorganisms like *S. maltophilia* and shows important components inside the EPS. Different DNases, glycosidases, and proteases were already described to attack the main components, like nucleic acids, polysaccharides, and proteins (Saggu et al.,



2019, Algburi et al., 2017). The study Elchinger et al. (2014) showed proteases that can be applied in an early stage of biofilm formation. Extracts of a flavourzyme and a neutrase were effective against *Staphylococcus epidermidis* and partly against *Staphylococcus aureus* biofilm. Especially the degradation of matrix proteins, like protein A, fibrinogen-binding proteins, and clumping factor B, and the associated destabilization of the biofilm is a target-oriented strategy (Saggu et al., 2019, Lister and Horswill 2014). Matrix metalloproteases (MMPs) are known to disintegrate parts of human extracellular matrices (Rowan et al., 2008, Pardo et al., 2008). Glycoproteins, like collagen and elastin, are useful points of action (Cui et al., 2017). For example, the bacterium *Microbacterium* sp. SKS10 secretes a metalloprotease able to remove *S. aureus* biofilm (Saggu et al., 2019). There is evidence for a human matrix metalloprotease, more precisely a collagenase, that prevents and degrades *Enterococcus faecalis* biofilm effectively (Kumar et al., 2019).

#### **4.4 Metalloproteases as promising anti-biofilm agents**

Our secretome evaluation led to a number of 185 potential proteases in the supernatant of the *M. foliosa* enrichment culture. The fractionation of the supernatant and further LC-MS/MS analysis of two fractions resulted in the identification of a putative metalloprotease. This enzyme could be comparable to ColA from *Bacillus cereus*, a secreted collagenase known for gelatinolytic activity against native tropocollagen (Abfalter et al., 2016). There is a series of pathogenic microorganisms, like *Vibrio alginolyticus* and *Streptococcus gordonii*, producing collagenases (Abfalter et al., 2016, Watanabe 2004). Predominantly, this group of metalloproteases also attacks eukaryotic matrix components (Apte and Parks et al., 2015). However, there are some studies that revealed that proteases e.g. from the MEROPS family 23, can disrupt the cell walls of other bacteria and thus are suitable as an antimicrobial agent (Nilsen et al., 2003, Ahmed et al., 2003).

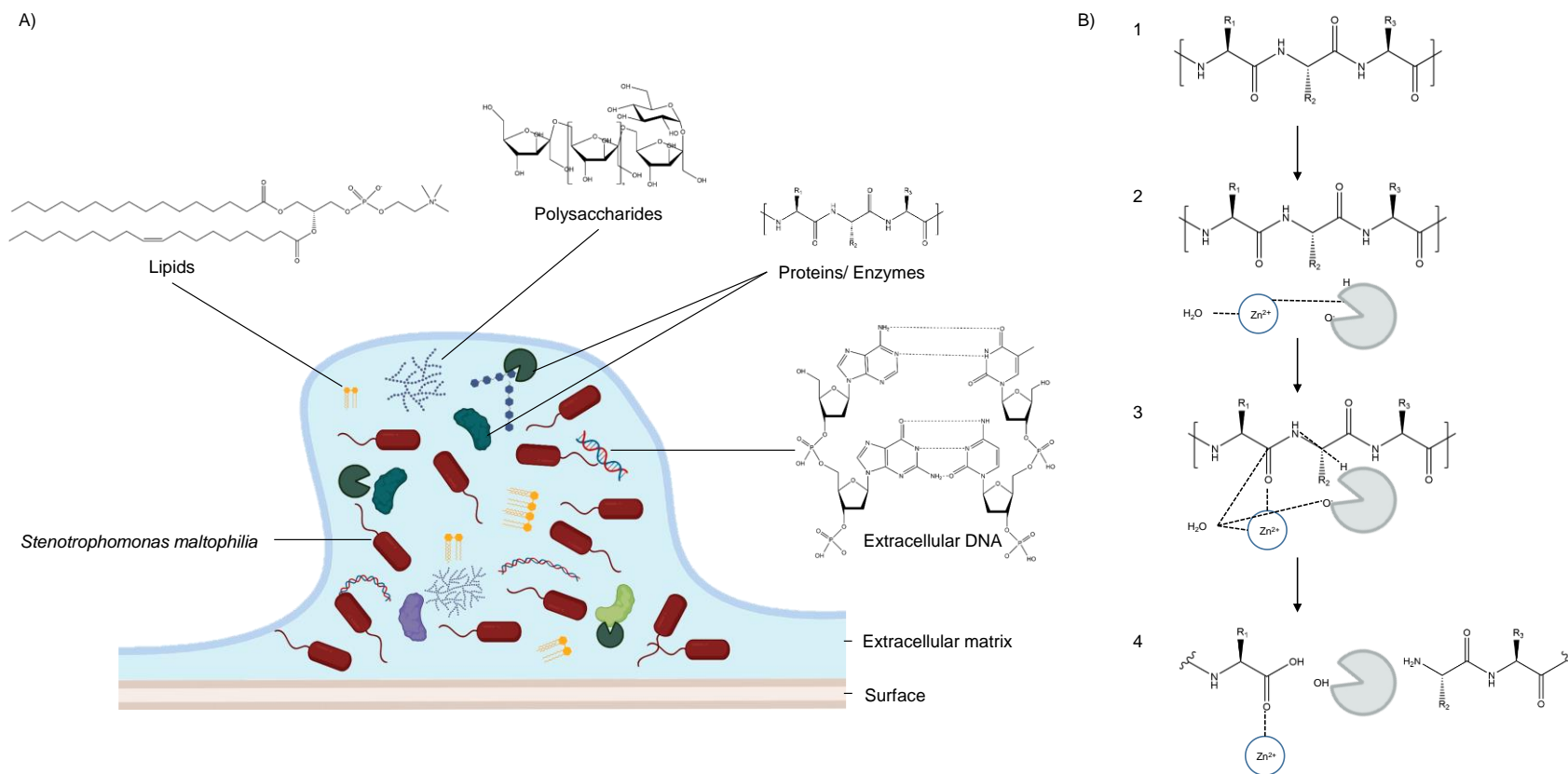


**Figure 15: Schematic model of *S. maltophilia* biofilm including compounds, and proposed mechanism of metalloproteases.** A) model of *S. maltophilia* K279a biofilm structure including selected extracellular polymeric substances of lipids (structure: phosphatidylcholin), polysaccharides (structure: levan), proteins/enzymes, and extracellular DNA. B) General mechanism of metalloproteases (modified, based on Hofmann, 1985; Elsässer and Goettig, 2021) 1. General peptide structure with R1-R3 representing side chain specifying the amino acid, serving as substrate for the metalloproteases. 2. A water molecule is kept in place by a zinc-(II)-cation which bonded on histidine of the metalloprotease. The endometalloprotease (grey enzyme) with an oxygen-(I)-anion and hydrogen-ion degrades the peptide bond. 3. When the substrate protein interacts with the enzyme, the zinc-(II)-cation binds to the carboxyl group of the substrate amino acid. The hydrogen of the enzyme bonds to the nitrogen of the amino acid, while the hydroxidion of the water molecule binds to the resulting free carbon. The remaining hydrogen binds to the oxygen-(I)-anion of the metalloprotease. 4. Degradation products. ChemDraw 21.0.0.28 (<https://perkinelmerinformatics.com>) was used for drawing, displaying, and characterizing chemical structures, substructures, and reactions. Biofilm and biological components were created with BioRender.com (original figure from Peters et al., 2023).

The cleavage of a peptide by metalloproteases is schematically represented in Figure 15B. Basically, it consists of three steps: A zinc-(II)-cation bonded on histidine of the metalloprotease kept a water molecule in position. The zinc-(II)-cation binds to the carboxyl group of the peptide and the hydrogen of the enzyme bonds to the nitrogen of the amino acid. While the hydroxidion of the water molecule binds to the resulting free carbon, the remaining hydrogen binds to the oxygen-(I)-anion of the metalloprotease (Peters et al., 2023, Hofman, 1985, Elsässer and Goettig, 2021).

#### **4.5 Conclusion and outlook**

In summary, with the great potential of samples from the marine environment, I identified a bacterial metalloprotease with convincing biofilm prevention activity against a human pathogen. The metalloprotease was effective against the biofilm formation of *S. maltophilia* K279a in an early phase. The confocal images validated a detachment of cells and destruction of the dense film. The analysis of the live and dead cells proved a clear reduction of the biofilm thickness.

Possibly, it could be applied to prevent the successful attachment of biofilms of various strains. Thereby the cells of these microorganisms can be attacked more effectively. The marine environment and its inhabitants provide great potential for exploring new enzymes for the pharmaceutical section. This study confirms that this kind of research brings us closer to a solution to serious health problems like multi-resistant microorganisms and chronic diseases.

The next step in this project would be the expression of individual proteases and the confirmation of the anti-biofilm activity. The results of the proteome analysis and the dataset of the coral metagenome could be compared, and the corresponding sequences could be used for cloning. Since the proteases probably originate from *Bacillus cereus*, a *Bacillus* strain would be a suitable cloning and expression system. Additionally, the structure of the biofilm should be investigated in a flowing system to imitate the natural conditions.

The results of this study provide a basis for further investigations on anti-biofilm enzymes and indicate that a deeper analysis of microbial products from the marine environment would be beneficial.

## 5 References

- Aaltonen E.K.J. and Silow M. (2008). "Transmembrane topology of the Acr3 family arsenite transporter from *Bacillus subtilis*." Biochim Biophys Acta **1778**, 963-973.
- Abda E.M., Krysciak D., Krohn-Molt I., Mamat U., Schmeisser C., Förstner K.U., Schaible U.E., Kohl T.A., Nieman S., and Streit W.R. (2015). "Phenotypic Heterogeneity Affects *Stenotrophomonas maltophilia* K279a Colony Morphotypes and  $\beta$ -Lactamase Expression." Front Microbiol **6**, 1373.
- Abfalter, C.M., Schönauer, E., Ponnuraj, K., Huemer, M., Gadermaier, G., Regl, C., Briza, P., Ferreira, F., Huber, C.G., Brandstetter, H., Posselt, G., and Wessler, S. (2016). "Cloning, Purification and Characterization of the Collagenase ColA Expressed by *Bacillus cereus* ATCC 14579." PLoS One **11**, e0162433.
- AboZahra, R. (2013). "Quorum Sensing and Interspecies Interactions in *Stenotrophomonas maltophilia*." Br Microbiol Res J **3**, 414-422.
- Ahmed K., Chohnan S., Ohashi H., Hirata T., Masaki T., and Sakiyama F. (2003). "Purification, Bacteriolytic Activity, and Specificity of  $\beta$ -Lytic Protease from *Lysobacter* sp. IB-9374." J Biosci Bioeng **95**, 27-34.
- Algburi A., Comito N., Kashtanov D., Dicks L.M.T., and Chikindas M.L. (2017). "Control of Biofilm Formation: Antibiotics and Beyond." Appl Environ Microbiol **83**, e02508-16.
- Alio I., Gudzuhn M., Pérez García P., Danso D., Schoelmerich M.C., Mamat U., Schaible U.E., Steinmann J., Yero D., Gibert I., Kohl T.A., Niemann S., Gröschel M.I., Haerdter J., Hackl T., Vollstedt C., Bömeke M., Egelkamp R., Daniel R., Poehlein A., and Streit W.R. (2020). "Phenotypic and Transcriptomic Analyses of Seven Clinical *Stenotrophomonas maltophilia* Isolates Identify a Small Set of Shared and Commonly Regulated Genes Involved in the Biofilm Lifestyle." Appl Environ Microbiol **86**, e02038-20.
- Alma'abadi A.D., Gojobori T., and Mineta K. (2015). "Marine Metagenome as A Resource for Novel Enzymes." Genom Proteom Bioinf **13**, 290-295.
- Angus, D.C., and van der Poll, T. (2013). "Severe Sepsis and Septic Shock." N Engl J Med **369**, 840-851.

- Anton A., Große C., Reißmann J., Pribyl T., and Nies D.H. (1999). "CzcD Is a Heavy Metal Ion Transporter Involved in Regulation of Heavy Metal Resistance in *Ralstonia* sp. Strain CH34." J Bacteriol **181**, 6876-6881.
- Apte S.S., and Parks W.C. (2015). "Metalloproteinases: A parade of functions in matrix biology and an outlook for the future." Matrix Biol **44-46**, 1-6.
- Barber C.E., Tang J.L., Feng J.X., Pan M.Q., Wilson T.J.G., Slater H., Dow J.M., Williams P., and Daniels M.J. (1997). "A novel regulatory system required for pathogenicity of *Xanthomonas campestris* is mediated by a small diffusible signal molecule." Mol Microbiol **24**, 555-566.
- Baslé A., Hewitt L., Koh A., Lamb H.K., Thompson P., Burgess J.G., Hall M.J., Hawkins A.R., Murray H., and Lewis R.J. (2017). "Crystal structure of NucB, a biofilm-degrading endonuclease." Nucleic Acids Res **46**, 473-484.
- Bayona, L. M., de Voogd, N. J., and Choi, Y. H. (2022). "Metabolomics on the study of marine organisms." Metabolomics **18**, 17.
- Berlutti F., Morea C., Battistoni A., Sarli S., Cipriani P., Superti F., Ammendolia M.G., and Valenti P. (2005). "Iron availability influences aggregation, biofilm, adhesion and invasion of *Pseudomonas aeruginosa* and *Burkholderia cenocepacia*." Int J Immunopathol Pharmacol **18**, 661-670.
- Bin Hafeez A., Jiang X., Bergen P.J., and Zhu Y. (2021). „Antimicrobial Peptides: An Update on Classifications and Databases." Int J Mol Sci **22**, 21, 11691.
- Brooke J.S. (2012). "*Stenotrophomonas maltophilia*: an Emerging Global Opportunistic Pathogen." Clin Microbiol Rev **25**, 2-41.
- Brooke J.S., Di Bonaventura G., Berg G., and Martinez J.L. (2017). "Editorial: A Multidisciplinary Look at *Stenotrophomonas maltophilia*: An Emerging Multi-Drug-Resistant Global Opportunistic Pathogen." Front Microbiol **8**, 1511.
- Cacaci M., Martini C., Guarino C., Torelli R., Bugli F., and Sanguinetti M. (2019). "Graphene Oxide Coatings as Tools to Prevent Microbial Biofilm Formation on Medical Device." Adv Exp Med Biol **14**, 21-35.
- Cattò C., and Cappitelli F. (2019). "Testing Anti-Biofilm Polymeric Surfaces: Where to Start?" Int J Mol Sci **20**, 3794.
- Chakraborty K., Thilakan B., and Raola V. K. (2014). "Polyketide Family of Novel Antibacterial 7-O-methyl-5'-hydroxy-3'-heptenoate-Macrolactin from Seaweed-Associated *Bacillus subtilis* MTCC 10403." J Agric Food Chem **62**, 12194-12208.

- Chakraborty K., Thilakan B., Chakraborty R.D., Raola V. K., and Joy M. (2017). "O-heterocyclic derivatives with antibacterial properties from marine bacterium *Bacillus subtilis* associated with seaweed, *Sargassum myriocystum*." Appl Microbiol Biotechnol **101**, 569-583.
- Chen Y. H., Kuo J., Sung P.-J., Chang Y.-C., Lu M.-C., Wong T.-Y., Liu J.-K., Weng C.-F., Twan W.-H., and Kuo F.-W. (2012). "Isolation of marine bacteria with antimicrobial activities from cultured and field-collected soft corals." World J Microbiol Biotechnol **28**, 3269-3279.
- Chen Y., Liu S. A., Mou H., Ma Y., Li M., and Hu X. (2017). "Characterization of Lipopeptide Biosurfactants Produced by *Bacillus licheniformis* MB01 from Marine Sediments." Front Microbiol **8**, 871.
- Chiou S.-F., Kuo J., Wong T.-Y., Fan T.-Y., Tew K. S., Liu J.-K. (2010). "Analysis of the coral associated bacterial community structures in healthy and diseased corals from off-shore of southern Taiwan." J Environ Sci Health B **45**, 408-415.
- Conte M., Fontana E., Nebbioso A., and Altucci L. (2020). "Marine-Derived Secondary Metabolites as Promising Epigenetic Bio-Compounds for Anticancer Therapy." Mar Drugs **19**, 15.
- Crack J.C., Green J., Hutchings M.I., Thomson A.J., and Le Brun N.E. (2012). "Bacterial Iron-Sulfur Regulatory Proteins as Biological Sensor-Switches." Antioxid Redox Signal **17**, 1215-1231.
- Cragg G.M., and Newman D.J. (2005). "Biodiversity : A continuing source of novel drug leads." Pure Appl Chem **77**, 7-24.
- Crossman L.C., Gould V.C., Dow J.M., Vernikos G.S., Okazaki A., Sebahia M., Saunders D., Arrowsmith C., Carver T., Peters N., Adlem E., Kerhornou A., Lord A., Murphy L., Seeger K., Squares R., Rutter S., Quail M.A., Rajandream M.-A., Harris D., Churcher C., Bentley S.D., Parkhill J., Thomson N.R., and Avison M.B. (2008). "The complete genome, comparative and functional analysis of *Stenotrophomonas maltophilia* reveals an organism heavily shielded by drug resistance determinants." Genome Biol **9**, R74.
- Cui N., Hu M., and Khalil R.A. (2017). "Biochemical and Biological Attributes of Matrix Metalloproteinases." Prog Mol Biol Transl Sci **147**, 1-73.
- Culp E., and Wright G.D. (2017). "Bacterial proteases, untapped antimicrobial drug targets." J Antibiot (Tokyo) **70**, 366-377.

- Darouiche R.O. (2004). "Treatment of Infections Associated with Surgical Implants." N Engl J Med **350**, 1422-1429.
- Díaz P.R., Torres M.J., Petroselli G., Erra-Balsells R., and Audisio M.C. (2022). "Antibacterial activity of *Bacillus licheniformis* B6 against viability and biofilm formation of foodborne pathogens of health importance." World J Microbiol Biotechnol **38**, 181.
- Diggle S.P., and Whiteley M. (2020). "Microbe Profile: *Pseudomonas aeruginosa*: opportunistic pathogen and lab rat." Microbiology (Reading) **166**, 30-33.
- Driscoll J.A., Brody S.L., and Kollef M.H. (2007). "The Epidemiology, Pathogenesis and Treatment of *Pseudomonas aeruginosa* Infections." Drugs **67**, 351-368.
- Eckhard U., Schönauer E., and Brandstetter H. (2013). "Structural Basis for Activity Regulation and Substrate Preference of Clostridial Collagenases G, H, and T." J Biol Chem **288**(28), 20184-20194.
- Elborn J.S. (2016). "Cystic fibrosis." Lancet **388**, 2519-2531.
- Elchinger P.-H., Delattre C., Faure S., Roy O., Badel S., Bernardi T., Taillefumier C., and Michaud P. (2014). "Effect of proteases against biofilms of *Staphylococcus aureus* and *Staphylococcus epidermidis*." Lett Appl Microbiol **59**, 507-513.
- El-Gendy M.M.A., Shaaban M., Shaaban K.A., El-Bondkly A.M., and Laatsch H. (2008). "Essramycin: A First Triazolopyrimidine Antibiotic Isolated from Nature" J Antibiot **61**, 149-157.
- Elsässer B., and Goettig P. (2021). "Mechanisms of Proteolytic Enzymes and Their Inhibition in QM/MM Studies." Int J Mol Sci **22**, 3232.
- Farasin J., Koechler S., Varet H., Deschamps J., Dillies M.A., Proux C., Erhardt M., Huber A., Jagla B., Briandet R., Coppée J.-Y., and Arsène-Ploetze F. (2017). "Comparison of biofilm formation and motility processes in arsenic-resistant *Thiomonas* spp. strains revealed divergent response to arsenite." Microb Biotechnol **10**, 789-803.
- Felsenstein J. (1985). "Confidence Limits on Phylogenies: An Approach using the Bootstrap." Evolution **39**, 783-791.
- Ferrer M., Beloqui A., Timmis K.N., and Golyshin P.N. (2008). "Metagenomics for Mining New Genetic Resources of Microbial Communities." J Mol Microbiol Biotechnol **16**, 109-123.
- Firn R.D., and Jones C.G. (2000). "The evolution of secondary metabolism – a unifying model." Mol Microbiol **37**, 989-994.

- Fjell C.D., Hiss J.A., Hancock R.E.W., and Schneider G. (2012). "Designing antimicrobial peptides: form follows function." Nat Rev Drug Discov **11**, 37-51.
- Fleming D., and Rumbaugh K.P. (2017). "Approaches to Dispersing Medical Biofilms." Microorganisms **5**, 15.
- Flemming H.C., Wingender J., Szewzyk U., Steinberg P., Rice S.A., and Kjelleberg S. (2016). „Biofilms: an emergent form of bacterial life." Nat Rev Microbiol **14**, 563-575.
- Flemming H.C., van Hullebusch E.D., Neu T.R., Nielsen P.H., Seviour T., Stoodley P., Wingender J., and Wuertz S. (2022). "The biofilm matrix: multitasking in a shared space." Nat Rev Microbiol **21**, 70-86.
- Fujita M., Mori K., Hara H., Hishiyama S., Kamimura N., and Masai E. (2019). "A TonB-dependent receptor constitutes the outer membrane transport system for a lignin-derived aromatic compound." Commun Biol **2**, 432.
- Garbinski L.D., Rosen B.P., and Chen J. (2019). "Pathways of arsenic uptake and efflux." Environ Int **126**, 585-597.
- Ghosh D., Seth M., Mondal P., and Mukhopadhyay S.K. (2022). "Bacterial biofilms: role of quorum sensing and quorum quenching." J Exp Biol Agric Sci **10**, 278-293.
- Giordano D. (2021). "Bioactive Molecules from Extreme Environments II." Mar Drugs **19**, 642.
- Giri S.S., Ryu E.C., Sukumaran V., and Park S.C. (2019). "Antioxidant, antibacterial, and anti-adhesive activities of biosurfactants isolated from *Bacillus* strains." Microb Pathog **132**, 66-72.
- Goodman J.K., Zampronio C.G., Jones A.M.E., and Hernandez-Fernaund J.R. (2018). "Updates of the In-Gel Digestion Method for Protein Analysis by Mass Spectrometry." Proteomics **18**, e1800236.
- Gotesman M., Wang Y., Madasu S.C., and Mitchell C.A. (2021). "Purification of Cytoskeletal Proteins by Fast Protein Liquid Chromatography (FPLC) Using an ÄKTA Start System." Methods Mol Biol **2364**, 1170.
- Grace A., Sahu R., Owen D.R., and Dennis V.A. (2022). "*Pseudomonas aeruginosa* reference strains PAO1 and PA14: A genomic, phenotypic, and therapeutic review." Front Microbiol **13**, 1023523.
- Guendouze A., Plener L., Bzdrenga J., Jacquet P., Rémy B., Elias M., Lavigne J.-P., Daudé D., and Chabrière E. (2017). "Effect of Quorum Quenching Lactonase in



- Clinical Isolates of *Pseudomonas aeruginosa* and Comparison with Quorum Sensing Inhibitors." Front Microbiol **8**, 227.
- Guo Y., Song G., Sun M., Wang J., and Wang Y. (2020). "Prevalence and Therapies of Antibiotic-Resistance in *Staphylococcus aureus*." Front Cell Infect Microbiol **10**, 107.
- Hancock R.E.W., and Sahl H.-G. (2006). "Antimicrobial and host-defense peptides as new anti-infective therapeutic strategies." Nat Biotechnol **24**, 1551-1557.
- Hancock R.E.W., and Speert D.P. (2000). "Antibiotic resistance in *Pseudomonas aeruginosa*: mechanisms and impact on treatment." Drug Resist Updat **3**, 247-255.
- Hansen C.R. (2012). "*Stenotrophomonas maltophilia*: to be or not to be a cystic fibrosis pathogen." Curr Opin Pulm Med **18**, 628-631.
- Hartmann R., Jeckel H., Jelli E., Singh P.K., Vaidya S., Bayer M., Rode D.K.H., Vidakovic L., Díaz-Pascual F., Fong J.C.N., Dragoš A., Lamprecht O., Thöming J.G., Netter N., Häussler S., Nadell C.D., Sourjik V., Kovács Á.T., Yildiz F.H., and Drescher K. (2021). "Quantitative image analysis of microbial communities with BiofilmQ." Nat Microbiol **6**, 151-156.
- Hoelt S.E., Kulp T.R., Han S., Lanoil B., and Oremland R.S. (2010). "Coupled Arsenotrophy in a Hot Spring Photosynthetic Biofilm at Mono Lake, California." Appl Environ Microbiol **76**, 4633-4639.
- Hofmann T. (1985). "Metalloproteinases. In Fuller, W., Neidle, S., and Harrison, P.M.. Topics in Molecular and Structural Biology, Metalloproteins – Part 2: Metal Proteins with Non-redox Roles." Published in Chemie ISBN 3-527-26137-0.
- Hohmann C., Schneider K., Bruntner C., Irran E., Nicholson G., Bull A.T., Jones A.L., Brown R., Stach J.E.M., Goodfellow M., Beil W., Krämer M., Imhoff J.F., Süssmuth R.D., and Fiedler H.-P. (2009). "Caboxamycin, a new antibiotic of the benzoxazole family produced by the deep-sea strain *Streptomyces* sp. NTK 937." J Antibiot (Tokyo) **62**, 99-104.
- Højby N., Ciofu O., Johansen H.K., Song Z.-J., Moser C., Jensen P.Ø., Molin S., Givskov M., Tolker-Nielsen T., and Bjarnsholt T. (2011). "The clinical impact of bacterial biofilms." Int J Oral Sci **3**, 55-65.
- Huedo P., Coves X., Daura X., Gibert I., and Yero D. (2018). "Quorum Sensing Signaling and Quenching in the Multidrug-Resistant Pathogen *Stenotrophomonas maltophilia*." Front Cell Infect Microbiol **8**, 122.

- Islam M.M., Kim K., Lee J.C., and Shin M. (2021). "LeuO, a LysR-Type Transcriptional Regulator, Is Involved in Biofilm Formation and Virulence of *Acinetobacter baumannii*." Front Cell Infect Microbiol **11**, 738706.
- Isom C.M., Blake F., and Anderson G.G. (2022). "Evaluating Metabolic Pathways and Biofilm Formation in *Stenotrophomonas maltophilia*." J Bacteriol **204**, e00398-21.
- Jamal M., Ahmad W., Andleeb S., Jalil F., Imran M., Nawaz M.A., Hussain T., Ali M., Rafiq M., and Kamil M.A. (2018). "Bacterial biofilm and associated infections." J Chin Med Assoc **81**, 7-11.
- Jones D.T., Tavlour W.R., and Thornton J.M. (1992). "The rapid generation of mutation data matrices from protein sequences." Comput Appl Biosci **8**, 275-82.
- Kang D., and Kirienko N.V. (2018). "Interdependence between iron acquisition and biofilm formation in *Pseudomonas aeruginosa*." J Microbiol **56**, 449-457.
- Kang H.K., Kim C., Seo C.H., and Park Y. (2017). "The therapeutic applications of antimicrobial peptides (AMPs): a patent review." J Microbiol **55**, 1-12.
- Kaplan J.B., Velliyagounder K., Ragonath C., Rohde H., Mack D., Knobloch J.K.-M, and Ramasubbu N. (2004). "Genes Involved in the Synthesis and Degradation of Matrix Polysaccharide in *Actinobacillus actinomycetemcomitans* and *Actinobacillus pleuropneumoniae* Biofilms." J Bacteriol **186**, 8213-8220.
- Kasari V., Mets T., Tenson T., and Kaldalu N. (2013). "Transcriptional cross-activation between toxin-antitoxin systems of *Escherichia coli*." BMC Microbiol **13**, 45.
- Khorchid A., and Ikura M. (2006). "Bacterial histidine kinase as signal sensor and transducer." Int J Biochem Cell Biol **38**, 307-312.
- König G.M., Kehraus S., Seibert S.F., Abdel-Lateff A., and Müller D. (2006). "Natural Products from Marine Organisms and Their Associated Microbes." ChemBioChem **7**, 229-238.
- Krueger F. (2012). "Trim Galore: a wrapper tool around Cutadapt and FastQC to consistently apply quality and adapter trimming to FastQ files, with some extra functionality for MspI-digested RRBS-type (Reduced Representation Bisulfite-Seq) libraries." URL <http://www.bioinformatics.babraham.ac.uk/projects/trimgalore/>.
- Kumar A., Alam A., Rani M., Ehtesham N.Z., and Hasnain S.E. (2017). "Biofilms: Survival and defense strategy for pathogens." Int J Med Microbiol **307**, 481-489.

- Kumar L., Cox C.R., and Sarkar S.K. (2019). "Matrix metalloprotease-1 inhibits and disrupts *Enterococcus faecalis* biofilms." PLoS One **14**, e0210218.
- Kumar S., Stecher G., Li M., Knyaz C., and Tamura K. (2018). "MEGA X: Molecular Evolutionary Genetics Analysis across Computing Platforms." Mol Biol Evol **35**, 1547-1549.
- Kurhekar J.V. (2020). "Antimicrobial lead compounds from marine plants." In *Phytochemicals as Lead Compounds for New Drug Discovery*, pp. 257-274.
- Kwiecinski J.M., and Horswill A.R. (2020). *Staphylococcus aureus* bloodstream infections: pathogenesis and regulatory mechanisms." Curr Opin Microbiol **53**, 51-60.
- Laemmli U.K. (1970). "Cleavage of Structural Proteins during the Assembly of the Head of Bacteriophage T4." Nature **227**, 680-685.
- Lakhundi S., and Zhang K. (2018). "Methicillin-Resistant *Staphylococcus aureus*: Molecular Characterization, Evolution, and Epidemiology." Clin Microbiol Rev **31**, e00020-18.
- Langmead B. and Salzberg S.L. (2012). "Fast gapped-read alignment with Bowtie 2." Nat Methods **9**, 357-359.
- Lazzarini A., Cavaletti L., Toppo G., and Marinelli F. (2000). "Rare genera of actinomycetes as potential producers of new antibiotics". KAP **78**, 399-405.
- Li H., Handsaker B., Wysoker A., Fennell T., Ruan J., Homer N., Marth G., Abecasis G., Durbin R. and 1000 Genome Project Data Processing Subgroup (2009). "The Sequence Alignment/Map format and SAMtools." Bioinformatics **25**, 2078–2079.
- Lister J.L., and Horswill A.R. (2014). "*Staphylococcus aureus* biofilms: recent developments in biofilm dispersal." Front Cell Infect Microbiol **4**, 178.
- Looney W.J., Narita M., and Mühlemann K. (2009). "*Stenotrophomonas maltophilia*: an emerging opportunist human pathogen." Lancet Infect Dis **9**, 312-323.
- Lopanik N., Lindquist N., and Targett N. (2004). "Potent cytotoxins produced by a microbial symbiont protect host larvae from predation." Oecologia **139**, 131-139.
- Lordan S., Ross R.P., and Stanton C. (2011). "Marine Bioactives as Functional Food Ingredients: Potential to Reduce the Incidence of Chronic Diseases." Mar Drugs **9**, 1056-1100.

- Mahlapuu M., Håkansson J., Ringstad L., and Björn C. (2016). "Antimicrobial Peptides: An Emerging Category of Therapeutic Agents." Front Cell Infect Microbiol **6**, 194.
- Manivasagan P., Venkatesan J., Sivakumar K., and Kim S.-K. (2013). "Pharmaceutically active secondary metabolites of marine actinobacteria." Microbiol Res **169**, 262-278.
- Markowitz V.M., Chen I.-M.A., Palaniappan K., Chu K., Szeto E., Grechkin Y., Ratner A., Jacob B., Huang J., Williams P., Huntemann M., Anderson I., Mavromatis K., Ivanova N.N., and Kyrpides N.C. (2012). "IMG: the integrated microbial genomes database and comparative analysis system." Nucleic Acids Res **40**, D115-122.
- Matsushita O., and Okabe A. (2001). "Clostridial hydrolytic enzymes degrading extracellular components." Toxicon **39**(11), 1769-1780.
- Mishra R., Panda A.K., De Mandal S., Shakeel M., Bisht S.S., and Khan J. (2020). "Natural Anti-biofilm Agents: Strategies to Control Biofilm-Forming Pathogens." Front Microbiol **11**, 566325.
- Modolon F., Barno A.R., Villela H.D.M., and Peixoto R.S. (2020). "Ecological and biotechnological importance of secondary metabolites produced by coral-associated bacteria." J Appl Microbiol **129**, 1441-1457.
- Mulcahy L.R., Isabella V.M., and Lewis K. (2014). "*Pseudomonas aeruginosa* biofilms in disease." Microb Ecol **68**, 1-12.
- Mullan K.A., Bramberger L.M., Munday P.R., Goncalves G., Revote J., Mifsud N.A., Illing P.T., Anderson A., Kwan P., Purcell A.W., and Li C. (2021). "ggVolcanoR: A Shiny app for customizable visualization of differential expression datasets." Comput Struct Biotechnol J **19**, 5735-5740.
- Nilsen T., Nes I.F., and Holo H. (2003). "Enterolysin A, a Cell Wall-Degrading Bacteriocin from *Enterococcus faecalis* LMG 2333." Appl Environ Microbiol **69**, 2975-2984.
- Nithyanand P., Thenmozhi R., Rathna J., and Pandian S.K. (2010). "Inhibition of *Streptococcus pyogenes* Biofilm Formation by Coral-Associated Actinomycetes." Curr Microbiol **60**, 454-460.
- Noinaj N., Guillier M., Barnard T.J., and Buchanan S.K. (2010). "TonB-dependent transporters: regulation, structure, and function." Annu Rev Microbiol **64**, 43-60.

- Notredame C., Higgins D.G., and Heringa J. (2000). "T-Coffee: A Novel Method for Fast and Accurate Multiple Sequence Alignment." J Mol Biol **302**, 205-217.
- Padmavathi A.R., and Pandian S.K. (2014). "Antibiofilm Activity of Biosurfactant Producing Coral Associated Bacteria Isolated from Gulf of Mannar." Indian J Microbiol **54**, 376-382.
- Pang Z., Raudonis R., Glick B.R., Lin T.-J., and Cheng Z. (2018). "Antibiotic resistance in *Pseudomonas aeruginosa*: mechanisms and alternative therapeutic strategies." Biotechnol Adv **37**, 177-192.
- Pardo A., Selman M., and Kaminski N. (2008). "Approaching the degradome in idiopathic pulmonary fibrosis." Int J Biochem Cell Biol **40**, 1141-1155.
- Park H., Kim D.E., Ovchinnikov S., Baker D., and DiMaio F. (2018). "Automatic structure prediction of oligomeric assemblies using Robetta in CASP12." Proteins **86 Suppl 1**, 283-291.
- Pawelek P.D., Croteau N., Ng-Thow-Hing C., Khursigara C.M., Moiseeva N., Allaire M., and Coulton J.W. (2006). "Structure of TonB in Complex with FhuA, *E. coli* Outer Membrane Receptor." Science **312**, 1399-1402.
- Peixoto R.S., Rosado P.M., Leite D.C.A., Rosado A.S., and Bourne D.G. (2017). "Beneficial Microorganisms for Corals (BMC): Proposed Mechanisms for Coral Health and Resilience." Front Microbiol **8**, 341.
- Pereira L.B., Palermo B.R.Z., Carlos C., and Ottoboni L.M.M. (2017). "Diversity and antimicrobial activity of bacteria isolated from different Brazilian coral species." FEMS Microbiol Lett **364**.
- Peters M.K., Astafyeva Y., Han Y., Macdonald J.F.H., Indenbirken D., Nakel J., Virdi S., Westhoff G., Streit W.R., and Krohn I. (2023). "Novel marine metalloprotease – new approaches for inhibition of biofilm formation of *Stenotrophomonas maltophilia*." Appl Microbiol Biotechnol **107**, 7119–7134.
- Pettersen E.F., Goddard T.D., Huang C.C., Meng E.C., Couch G.S., Croll T.I., Morris J.H., and Ferrin T.E. (2021). "UCSF ChimeraX: Structure visualization for researchers, educators, and developers." Protein Sci **30**, 70-82.
- Popovic A., Tchigvintsev A., Tran H., Chernikova T.N., Golyshina O.V., Yakimov M.M., Golyshin P.N., and Yakunin A.F. (2015). "Metagenomics as a Tool for Enzyme Discovery: Hydrolytic Enzymes from Marine-Related Metagenomes." In Prokaryotic Systems Biology Krogan N.J., and Babu M., eds. Pp. 1-20.

- Prashith Kekuda T.R., Shobha K.S., and Onkarappa R. (2010). "Fascinating diversity and Potent biological activities of Actinomycete meatbolites." J Pharm Res **3**, 250-256.
- Prjibelski A., Antipov D., Meleshko D., Lapidus A., and Korobeynikov A. (2020). "Using SPAdes De Novo Assembler." Bioinformatics **70**, e102.
- Rogers S.A., Huigens R.W. 3<sup>rd</sup>, Cavanagh J., and Melander C. (2010). "Synergistic Effects between Conventional Antibiotics and 2-Aminoimidazole-Derived Antibiofilm Agents." Antimicrob Agents Chemother **54**, 2112-2118.
- Römling U., and Balsalobre C. (2012). "Biofilm infections, their resilience to therapy and innovative treatment strategies." J Intern Med **272**, 541-561.
- Rostami N., Shields R.C., Yassin S.A., Hawkins A.R., Bowen L., Luo T.L., Rickard A.H., Holliday R., Preshaw P.M., and Jakubovics N.S. (2017). "A Critical Role for Extracellular DNA in Dental Plaque Formation." J Dent Res **96**, 208-216.
- Rowan A.D., Litherland G.J., Hui W., and Milner J.M. (2008). "Metalloproteases as potential therapeutic targets in arthritis treatment." Expert Opin Ther Targets **12**, 1-18.
- Roy R., Tiwari M., Donelli G., and Tiwari V. (2018). "Strategies for combating bacterial biofilms: A focus on anti-biofilm agents and their mechanisms of action." Virulence **9**, 522-554.
- Saggu S.K., Jha G., and Mishra P.C. (2019). "Enzymatic Degradation of Biofilm by Metalloprotease From *Microbacterium* sp. SKS10." Front Bioeng Biotechnol **7**, 192.
- Sánchez M.B. (2015). "Antibiotic resistance in the opportunistic pathogen *Stenotrophomonas maltophilia*." Front Microbiol **6**, 658.
- Sayers E.W., Beck J., Bolton E.E., Bourexis D., Brister J.R., Canese K., Comeau D.C., Funk K., Kim S., Klimke W., Marchler-Bauer A., Landrum, M., Lathrop, S., Lu Z., Madden T.L., O'Leary N., Phan L., Rangwala S.H., Schneider, V.A., Skripchenko Y., Wang J., Ye J., Trawick B.W., Pruitt K.D., and Sherry S.T. (2021). "Database resources of the National Center for Biotechnology Information." Nucleic Acids Research **49**, D10-D17.
- Schägger H. (2006). "Tricine-SDS-PAGE." Nat Protoc **1**, 16-22.
- Sharma D., Misba L., and Khan A.U. (2019). "Antibiotics versus biofilm: an emerging battleground in microbial communities." Antimicrob Resist Infect Control **8**, 76.

- Sharma G., Rao S., Bansal A., Dang S., Gupta S., and Gabrani R. (2013). "Pseudomonas aeruginosa biofilm: Potential therapeutic targets." Biologicals **42**, 1-7.
- Shnit-Orland M., and Kushmaro A. (2009). "Coral mucus-associated bacteria: a possible first line of defense." FEMS Microbiol Ecol **67**, 371-380.
- Simon C., and Daniel R. (2011). "Metagenomic Analyses: Past and Future Trends." Appl Environ Microbiol **77**, 1153-1161.
- Singh P.K., Schaefer A.L., Parsek M.R., Moninger T.O., Welsh M.J., and Greenberg E.P. (2000). "Quorum-sensing signals indicate that cystic fibrosis lungs are infected with bacterial biofilms." Nature **407**, 762-764.
- Singh R., Kumar M., Mittal A., and Mehta P.K. (2016). "Microbial enzymes: industrial progress in 21st century." 3 Biotech **6**, 174.
- Steinberger R.E., and Holden P.A. (2005). "Extracellular DNA in Single- and Multiple-Species Unsaturated Biofilms." Appl Environ Microbiol **71**, 5404-5410.
- Steinmann J., Mamat U., Abda E.M., Kirchhoff L., Streit W.R., Schaible U.E., Niemann, S., and Kohl T.A. (2018). "Analysis of Phylogenetic Variation of *Stenotrophomonas maltophilia* Reveals Human-Specific Branches." Front Microbiol **9**, 806.
- Streit W.R., and Schmitz R.A. (2004). „Metagenomics - the key to the uncultured microbes." Curr Opin Microbiol **7**, 492-498.
- Subramenium G.A., Swetha T.K., Iyer P.M., Balamurugan K., and Pandian S.K. (2018). "5-hydroxymethyl-2-furaldehyde from marine bacterium *Bacillus subtilis* inhibits biofilm and virulence of *Candida albicans*." Microbiol Res **207**, 19-32.
- Sullivan M.J., Goh K.G.K., and Ulett G.C. (2021). "Cellular Management of Zinc in Group B *Streptococcus* Supports Bacterial Resistance against Metal Intoxication and Promotes Disseminated Infection." mSphere **6**, e00105-21.
- Teitzel G.M., and Parsek M.R. (2003). "Heavy Metal Resistance of Biofilm and Planktonic *Pseudomonas aeruginosa*." AEM **69**, 2313-2320.
- The UniProt Consortium (2021). "UniProt: the universal protein knowledgebase in 2021." Nucleic Acids Res **49**, D480-D489.
- Tolker-Nielsen T. (2015). "Biofilm Development." Microbiol Spectrum **3**.
- Tout J., Jeffries T.C., Petrou K., Tyson G.W., Webster N.S., Garren M., Stocker R., Ralph P.J., and Seymour J.R. (2015). "Chemotaxis by natural populations of coral reef bacteria." ISME J **9**, 1764-1777.

- Trapnell C., Roberts A., Goff L., Pertea G., Kim D., Kelley D.R., Pimentel H., Salzberg S.L., Rinn J.L., and Pachter L. (2012). "Differential gene and transcript expression analysis of RNA-seq experiments with TopHat and Cufflinks." Nat Protoc **7**, 562–578.
- Venkateskumar K., Parasuraman S., Chuen L.Y., Ravichandran V., and Balamurgan S. (2020). "Exploring Antimicrobials from the Flora and Fauna of Marine: Opportunities and Limitations." Curr Drug Discov Technol **17**, 507-514.
- Vilela C.L.S., Villela H.D.M., Rachid C.T.C.d.C., Carmo F.L.d., Vermelho A.B., and Peixoto R.S. (2021). „Exploring the Diversity and Biotechnological Potential of Cultured and Uncultured Coral-Associated Bacteria." Microorganisms **9**, 2235.
- Wang K., Li X., Yang C., Song S., Cui C., Zhou X., and Deng Y. (2021). "A LysR Family Transcriptional Regulator Modulates *Burkholderia cenocepacia* Biofilm Formation and Protease Production." AEM **87**, e00202-21.
- Wang X., and Wood T.K. (2011). "Toxin-Antitoxin Systems Influence Biofilm and Persister Cell Formation and the General Stress Response." Appl Environ Microbiol **77**, 5577-5583.
- Watanabe K. (2004). "Collagenolytic proteases from bacteria." Appl Microbiol Biotechnol **63**, 520-526.
- Wawrzycka D., Markowska K., Maciaszczyk-Dziubinska E., Migocka M., and Wysocki R. (2017). "Transmembrane topology of the arsenite permease Acr3 from *Saccharomyces cerevisiae*." Biochim Biophys Acta Biomembr **1859**, 117-125.
- Wertheim H.F.L., Melles D.C., Vos M.C., van Leeuwen W., van Belkum A., Verbrugh H.A., and Nouwen J.L. (2005). "The role of nasal carriage in *Staphylococcus aureus* infections." Lancet Infect Dis **5**, 751-762.
- Whitchurch C.B., Tolker-Nielsen T., Ragas P.C., and Mattick J.S. (2002). "Extracellular DNA Required for Bacterial Biofilm Formation." Science **295**, 1487.
- Wu J.-W., and Chen X.-L. (2011). "Extracellular metalloproteases from bacteria." Appl Microbiol Biotechnol **92**, 253-262.
- Xiao S., Chen N., Chai Z., Zhou M., Xiao C., Zhao S., and Yang X. (2022). "Secondary Metabolites from Marine-Derived *Bacillus*: A Comprehensive Review of Origins, Structures, and Bioactivities." Mar Drugs **20**, 567.
- Zhang Y., Pan X., Wang L., and Chen L. (2021). "Iron metabolism in *Pseudomonas aeruginosa* biofilm and the involved iron-targeted anti-biofilm strategies." J Drug Target **29**, 249-258.



## **6 Acknowledgments**

First, I would like to thank my supervisor Prof. Dr. Wolfgang Streit for guiding me through my doctoral studies and for the exchange of ideas. I would also like to thank my co-supervisor Dr. Ines Krohn who supported me throughout the entire time of my PhD.

I would like to thank the working group of Prof. Streit for the pleasant working atmosphere over the years. I miss my desk by the window, surrounded by very nice colleagues. I had a great time at the office of miracles with inspiring exchange of ideas, extensive coffee breaks, and crazy parties.

I would also like to thank my parents, my close family and friends who have supported and motivated me. Special thanks to Christoph, who always believed in me.